WADC TECHNICAL REPORT 55-192 Vol II
ASTIA DOCUMENT NO. AD 110408

STUDIES ON THERMAL STRESSES FOR AIRCRAFT STRUCTURES EXPOSED TO TRANSIENT EXTERNAL HEATING

VOLUME II

AN ANALYTICAL METHOD FOR THE PREDICTION OF THE BEHAVIOR OF A SHEET-STRINGER PANEL WITH A UNIFORMLY HEATED SURFACE

James E. Mahlmeister
Burton A. Lieb

University of California
Department of Engineering
Los Angeles 24, California

[redacted]

December 1955

Aircraft Laboratory
Contract No. AF 33(616)-293
Project No. 1350

Wright Air Development Center
Air Research and Development Command
United States Air Force
Wright-Patterson Air Force Base, Ohio

FOREWORD

This report was prepared by J. E. Mahlmeister and B. A. Lieb of the Department of Engineering, University of California, Los Angeles, under Contract No. AF 33(616)-293. The contract was initiated under Project No. 1350, "Effects of Atomic Weapons on Aircraft Systems," and was administered by the Aircraft Laboratory, Directorate of Laboratories, Wright Air Development Center, with Lt. Joseph W. Saylor, Jr., acting as project engineer.

Alphonso Ambrosio directed and was technically responsible for the research described in this report and Walter C. Hurty acted as the representative of the Chairman of the Department, L. M. K. Boelter.

The authors wish to acknowledge the valuable discussions with Messrs. A. Ambrosio and T. Ishimoto, the assistance of Mr. I. Grossman in performing the survey experiment, and the help given by Mr. J. W. Colin with the calculations during the preparation of this report.

ABSTRACT

This report is a study of the behavior of a sheet-stringer panel with a uniformly heated surface. The panel is idealized such that the heat conduction analysis can be combined with the elastic heated plate equations enabling prediction of the transient stresses and deflections. The results show that a limiting load occurs which corresponds to the Euler elastic buckling criterion for slender columns. A method for predicting high temperature inelastic buckling is also suggested.

PUBLICATION REVIEW

This report has been reviewed and is approved.

FOR THE COMMANDER:

for Carl Reichert

Daniel D. McKee
Colonel, U.S.A.F.
Chief, Aircraft Laboratory
Directorate of Laboratories

CONTENTS

LIST OF FIGURES

NOMENCLATURE

a_0 =	Original plate length in x - direction	in
a_h =	Heated plate length in x - direction	in
a =	Thermal diffusivity	ft^2/hr
A =	Cross-sectional area of plate	in^2
b =	Plate thickness	in
Bi =	Biot's modulus	dimensionless
c =	Parameter defined as $\sqrt{\frac{-N_x}{D_2}}$	in^{-1}
C_p =	Heat capacity	Btu/lb °F
D_0 =	Rigidity parameter defined by equation (17)	lb/in
D_1 =	Rigidity parameter defined by equation (18)	lb
D_2 =	Plate flexual rigidity defined by equation (19)	in lb
d =	Length of plate in y - direction	in
E =	Modulus of elasticity	lb/in^2
E_t, E_s =	Tangent modulus, secant modulus	lb/in^2
h_c =	Unit thermal conductance	Btu/hr ft^2 °F
I =	Moment of inertia of plate (about y - axis)	in^4
K =	Equivalent spring stiffness per unit length of plate	lb/in^2
k =	Thermal conductivity	Btu/hr ft^2 °F/ft
l =	Length of curved plate in the x - direction	in
M =	Moment per unit length of plate	lb in/in
M_T =	Thermal moment	lb in/in
N =	In-plane force per unit length of plate	lb/in
N_T =	Thermal force	lb/in
p =	Lateral pressure loading	lb/in^2
q =	Rate of heat flow per unit area into plate	Btu/hr ft^2

Q	=	Total heat absorbed by plate	Btu
T	=	Temperature rise	°F
t	=	Time	sec or hr
u, v, w	=	Displacements in the x, y, z directions, respectively	in
x, y, z	=	Coordinates	in
α	=	Coefficient of linear thermal expansion	$°F^{-1}$
β	=	Heat transfer parameter ($b/\sqrt{a\eta}$)	dimensionless
γ	=	Shear strain	in/in
δ	=	Change of length	in
Δ	=	Difference	--
ϵ	=	Strain	in/in
η	=	Reference time	sec or hr
θ	=	Constraint factor	in/lb
ν	=	Poisson's Ratio	dimensionless
ρ_0	=	Weight density	lb/ft^3
ρ	=	Radius of gyration	in
σ	=	Normal stress	lb/in^2
τ	=	Shear stress	lb/in^2
ϕ	=	Stress function defined by equation (34)	lb
ψ	=	System parameter defined by equation (74)	dimensionless

Subscripts

h	heated
Cr	critical
x, y, z	coordinates
o	initial or ambient
f	front surface

Superscripts

+	dimensionless
*	rigid constraints ($K = \infty$)
–	average

INTRODUCTION

Transient heating of structures induces stresses and deformations as a result of temperature distributions, particularly when thermal expansion is restrained. Because interrelation of the variables which affect these factors should be clearly understood for the formulation of design and performance criteria, an analytical study of a simplified system believed to be representative of a typical sheet-stringer panel was undertaken.

Previous studies[1,2*] of the thermal response characteristics of transient heating for aircraft structures have related the response characteristics of the system to its heat transfer parameters. It is well known that this heating can cause structural failure due to (1) excessive temperatures resulting in loss of strength and (2) excessive stresses. Other undesirable effects may be bowing out of the heated skin during the heating cycle and the possible permanent deformation which may occur during the cycle.

In order to further evaluate these effects the thermal solution for the finite plate [1] was utilized to analytically determine the so-called "thermal force" and "thermal moment." These results are reported in reference 3 and will be used for the evaluation of the transient deflections and stresses after the thermo-elastic relations are established.

Fortunately, it is possible to consider the thermo-elastic analysis as a static problem. This simplification, which neglects the inertial forces as shown in reference 12, makes it possible to specify the stress distribution at any instant for which the temperature distribution is known. Hence, it is seen that the thermo-elastic analysis can be made independently of the heat transfer analysis.

Specifically, it is the purpose of this report to analytically interrelate the heat transfer and thermal stress parameters for the simplified system which will be described. The analysis, as will be shown, leads to a method for the prediction of stresses, deflections and presence of permanent deformations of the structure.

---

* Superscript numbers refer to list of references at the end of the report.

SECTION I. HEATED PLATE EQUATIONS

1. General Equations

The thermal stress equations for isotropic heated plates have been presented by a number of authors[4,10,12]. The analyses presented in references 4, 10, and 12 are extended in reference 8 to include large deflections of isothermal plates. In this section the general equations referred to above have been modified and extended to include large deflections of non-isothermal plates.

The basic postulates, which were made in the development of the equations describing the behavior of the heated plates are:

1. Kirchoff's bending assumption - i.e., points initially lying on a normal to the middle plane remain on the normal to the deformed middle plane.
2. The thickness is small compared to other dimensions.
3. Plane state of stress.
4. Elastic behavior.

Based upon the above assumptions the relations between the strains and displacements are:

$$\epsilon_x = \frac{\partial u}{\partial x} + \frac{1}{2}\left(\frac{\partial w}{\partial x}\right)^2 - z\frac{\partial^2 w}{\partial x^2} \tag{1}$$

$$\epsilon_y = \frac{\partial v}{\partial y} + \frac{1}{2}\left(\frac{\partial w}{\partial y}\right)^2 - z\frac{\partial^2 w}{\partial y^2} \tag{2}$$

and

$$\gamma_{xy} = \frac{\partial u}{\partial y} + \frac{\partial v}{\partial x} + \frac{\partial w}{\partial x}\frac{\partial w}{\partial y} - 2z\frac{\partial^2 w}{\partial x \partial y} \tag{3}$$

These equations can be combined in the compatibility equation

$$\frac{\partial^2 \epsilon_x}{\partial y^2} + \frac{\partial^2 \epsilon_y}{\partial x^2} - \frac{\partial^2 \gamma_{xy}}{\partial x \partial y} = \left(\frac{\partial^2 w}{\partial x \partial y}\right)^2 - \frac{\partial^2 w}{\partial x^2}\frac{\partial^2 w}{\partial y^2} \tag{4}$$

The stress strain relations for the plane state of stress are

$$\sigma_x = \frac{E}{1-\nu^2}\left[\epsilon_x + \nu\epsilon_y - (1+\nu)\,\alpha T\right] \tag{5}$$

$$\sigma_y = \frac{E}{1-\nu^2}\left[\epsilon_y + \nu\epsilon_x - (1+\nu)\,\alpha T\right] \tag{6}$$

and $$\tau_{xy} = \frac{E}{2(1+\nu)}\,\gamma_{xy} \tag{7}$$

Substituting the strain-displacement relations (1), (2), and (3) into equations (5), (6), and (7) gives the local stress-displacement relations:

$$\sigma_x = \frac{E}{1-\nu^2}\left[\frac{\partial u}{\partial x} + \nu\frac{\partial v}{\partial y} + \frac{1}{2}\left(\frac{\partial w}{\partial x}\right)^2 + \frac{\nu}{2}\left(\frac{\partial w}{\partial y}\right)^2 - \left(\frac{\partial^2 w}{\partial x^2} + \nu\frac{\partial^2 w}{\partial y^2}\right)z - (1+\nu)\alpha T\right] \tag{8}$$

$$\sigma_y = \frac{E}{1-\nu^2}\left[\frac{\partial v}{\partial y} + \nu\frac{\partial u}{\partial x} + \frac{1}{2}\left(\frac{\partial w}{\partial y}\right)^2 + \frac{\nu}{2}\left(\frac{\partial w}{\partial x}\right)^2 - \left(\frac{\partial^2 w}{\partial y^2} + \nu\frac{\partial^2 w}{\partial x^2}\right)z - (1+\nu)\alpha T\right] \tag{9}$$

$$\tau_{xy} = \frac{E}{2(1+\nu)}\left[\frac{\partial u}{\partial y} + \frac{\partial v}{\partial x} + \frac{\partial w}{\partial x}\frac{\partial w}{\partial y} - 2z\,\frac{\partial^2 w}{\partial x\partial y}\right] \tag{10}$$

The local stresses are integrated over the plate thickness to obtain the sectional forces and moments.

$$N_x \equiv \int_{-b/2}^{b/2}\sigma_x\,dz = D_0\left[\frac{\partial u}{\partial x} + \nu\frac{\partial v}{\partial y}\right] + \frac{D_0}{2}\left[\left(\frac{\partial w}{\partial x}\right)^2 + \nu\left(\frac{\partial w}{\partial y}\right)^2\right] - D_1\left[\frac{\partial^2 w}{\partial x^2} + \nu\frac{\partial^2 w}{\partial y^2}\right] - N_T \tag{11}$$

$$N_y \equiv \int_{-b/2}^{b/2} \sigma_y \, dz = D_0 \left[\frac{\partial v}{\partial y} + \nu \frac{\partial u}{\partial x} \right] + \frac{D_0}{2} \left[\left(\frac{\partial w}{\partial y} \right)^2 + \nu \left(\frac{\partial w}{\partial x} \right)^2 \right]$$
$$- D_1 \left[\frac{\partial^2 w}{\partial y^2} + \nu \frac{\partial^2 w}{\partial x^2} \right] - N_T \tag{12}$$

$$N_{xy} \equiv \int_{-b/2}^{b/2} \tau_{xy} \, dz = \frac{1 - \nu}{2} \left[D_0 \left(\frac{\partial u}{\partial y} + \frac{\partial v}{\partial x} + \frac{\partial w}{\partial x} \frac{\partial w}{\partial y} \right) - 2 D_1 \frac{\partial^2 w}{\partial x \partial y} \right] \tag{13}$$

$$M_x \equiv \int_{-b/2}^{b/2} \sigma_x z \, dz = D_1 \left[\frac{\partial u}{\partial x} + \nu \frac{\partial v}{\partial y} \right] + \frac{D_1}{2} \left[\left(\frac{\partial w}{\partial x} \right)^2 + \nu \left(\frac{\partial w}{\partial y} \right)^2 \right]$$
$$- D_2 \left[\frac{\partial^2 w}{\partial x^2} + \nu \frac{\partial^2 w}{\partial y^2} \right] - M_T \tag{14}$$

$$M_y \equiv \int_{-b/2}^{b/2} \sigma_y \, z \, dz = D_1 \left[\frac{\partial v}{\partial y} + \nu \frac{\partial u}{\partial x} \right] + \frac{D_1}{2} \left[\left(\frac{\partial w}{\partial y} \right)^2 + \nu \left(\frac{\partial w}{\partial x} \right)^2 \right]$$
$$- D_2 \left[\frac{\partial^2 w}{\partial y^2} + \nu \frac{\partial^2 w}{\partial x^2} \right] - M_T \tag{15}$$

and $$M_{xy} \equiv \int_{-b/2}^{b/2} z \, \tau_{xy} \, dz = \frac{1 - \nu}{2} \left[D_1 \left(\frac{\partial u}{\partial y} + \frac{\partial v}{\partial x} + \frac{\partial w}{\partial x} \frac{\partial w}{\partial y} \right) - 2 D_2 \frac{\partial^2 w}{\partial x \partial y} \right] \tag{16}$$

where the following definitions were employed:

$$D_0 \equiv \frac{1}{1 - \nu^2} \int_{-b/2}^{b/2} E \, dz \tag{17}$$

$$D_1 \equiv \frac{1}{1 - \nu^2} \int_{-b/2}^{b/2} E z \, dz \tag{18}$$

$$D_2 \equiv \frac{1}{1 - \nu^2} \int_{-b/2}^{b/2} E z^2 \, dz \tag{19}$$

$$N_T \equiv \frac{1}{1-\nu} \int_{-b/2}^{b/2} E \alpha T \, dz \qquad (20)^*$$

and

$$M_T \equiv \frac{1}{1-\nu} \int_{-b/2}^{b/2} E \alpha T z \, dz \qquad (21)^*$$

Setting $D_1 = 0$ in equation (18) establishes the location of the neutral surface and allows considerable simplification of equations (11) through (16). Equation (19) becomes the usual expression for the plate flexural rigidity if Young's Modulus does not vary across the thickness. Setting $D_1 = 0$, equations (11) through (16) become

$$N_x = D_0 \left[\frac{\partial u}{\partial x} + \nu \frac{\partial v}{\partial y} \right] + \frac{D_0}{2} \left[\left(\frac{\partial w}{\partial x} \right)^2 + \nu \left(\frac{\partial w}{\partial y} \right)^2 \right] - N_T \qquad (22)$$

$$N_y = D_0 \left[\frac{\partial v}{\partial y} + \nu \frac{\partial u}{\partial x} \right] + \frac{D_0}{2} \left[\left(\frac{\partial w}{\partial y} \right)^2 + \nu \left(\frac{\partial w}{\partial x} \right)^2 \right] - N_T \qquad (23)$$

$$N_{xy} = D_0 \frac{1-\nu}{2} \left[\frac{\partial u}{\partial y} + \frac{\partial v}{\partial x} + \frac{\partial w}{\partial x} \frac{\partial w}{\partial y} \right] \qquad (24)$$

$$M_x = - D_2 \left[\frac{\partial^2 w}{\partial x^2} + \nu \frac{\partial^2 w}{\partial y^2} \right] - M_T \qquad (25)$$

$$M_y = - D_2 \left[\frac{\partial^2 w}{\partial y^2} + \nu \frac{\partial^2 w}{\partial x^2} \right] - M_T \qquad (26)$$

---

*N_T and M_T are referred to as the thermal force and thermal moment, respectively.

and $$M_{xy} = -D_2(1-\nu)\frac{\partial^2 w}{\partial x \partial y} \qquad (27)$$

Local stresses in terms of the sectional forces and moments are obtained by substituting equations (22) and (25) into equation (8), equations (23) and (26) into equation (9), and equations (24) and (27) into equation (10).

$$\sigma_x = \frac{E}{1-\nu^2}\left[\frac{N_x + N_T}{D_0} - \frac{M_x + M_T}{D_2} z - (1+\nu)\,\alpha T\right] \qquad (28)$$

$$\sigma_y = \frac{E}{1-\nu^2}\left[\frac{N_y + N_T}{D_0} - \frac{M_y + M_T}{D_2} z - (1+\nu)\,\alpha T\right] \qquad (29)$$

and

$$\tau_{xy} = \frac{E}{1-\nu^2}\left[\frac{N_{xy}}{D_0} + \frac{M_{xy}}{D_2} z\right] \qquad (30)$$

It is interesting to note that equations (28) and (29) reduce to those given in reference 9 if N_x, N_y, M_x and M_y are zero. This corresponds to the case of an unrestrained heated plate.

The sectional forces and moments are obtained from the above relations and the equations of equilibrium which are

$$\frac{\partial N_x}{\partial x} + \frac{\partial N_{xy}}{\partial y} = 0 \qquad (31)$$

$$\frac{\partial N_y}{\partial y} + \frac{\partial N_{xy}}{\partial x} = 0 \qquad (32)$$

and

$$\frac{\partial^2 M_x}{\partial x^2} - 2\frac{\partial^2 M_{xy}}{\partial x \partial y} + \frac{\partial^2 M_y}{\partial y^2} = -p - N_x\frac{\partial^2 w}{\partial x^2} - 2N_{xy}\frac{\partial^2 w}{\partial x \partial y} - N_y\frac{\partial^2 w}{\partial y^2} \qquad (33)$$

Equations (31) and (32) can be satisfied identically by defining the stress function

$$N_x = b\,\frac{\partial^2\phi}{\partial y^2}\,, \quad N_y = b\,\frac{\partial^2\phi}{\partial x^2} \quad \text{and } N_{xy} = -b\,\frac{\partial^2\phi}{\partial x\partial y} \tag{34}$$

With this definition the compatibility equation (4) becomes

$$\frac{\partial^4\phi}{\partial x^4} + 2\,\frac{\partial^4\phi}{\partial y^2\partial x^2} + \frac{\partial^4\phi}{\partial y^4} = E\left[\left(\frac{\partial^2 w}{\partial x\partial y}\right)^2 - \frac{\partial^2 w}{\partial x^2}\,\frac{\partial^2 w}{\partial y^2}\right]$$

$$- \frac{1-\nu}{b}\left[\frac{\partial^2 N_T}{\partial x^2} + \frac{\partial^2 N_T}{\partial y^2}\right]$$

or

$$\nabla^4\phi = E\left[\left(\frac{\partial^2 w}{\partial x\partial y}\right)^2 - \frac{\partial^2 w}{\partial x^2}\,\frac{\partial^2 w}{\partial y^2}\right] - \frac{1-\nu}{b}\,\nabla^2 N_T \tag{35}$$

Combining equations (14), (15) and (16) with equation (33) leads to

$$D_2\nabla^4 w = +\,p - \nabla^2 M_T + b\left[\frac{\partial^2\phi}{\partial y^2}\,\frac{\partial^2 w}{\partial x^2} - 2\,\frac{\partial^2\phi}{\partial x\partial y}\,\frac{\partial^2 w}{\partial x\partial y} + \frac{\partial^2\phi}{\partial x^2}\,\frac{\partial^2 w}{\partial y^2}\right] \tag{36}$$

In the general case it is necessary to solve equations (35) and (36) simultaneously with appropriate boundary conditions. The in-plane forces and moments are then determined from solutions for the deflection w and the stress function ϕ. Finally the local stresses may be obtained from equations (28), (29) and (30).

2. Solution for the Simplified System

The analysis presented above is perfectly general. However, a solution to the general case has not been obtained due to the complexity of equations (35) and (36). In the following pages these equations are made amenable to solution by applying them to a particular system, i.e., a sheet-stringer panel. The ensuing simplification of the equations allows calculation of the significant stresses and deflections.

Figure 1 shows a section of a typical sheet-stringer panel. Usually the spacing between ribs is many times the distance between stringers. The aerodynamic load which would be principally a tensile or compressive load in the y-direction and a pressure load p in the z-direction is not considered in this analysis. The induced loads due to restrained thermal expansion will cause the stringers to be displaced in a chordwise direction, the load being ultimately reacted against the spars. The actual load will be related to the elastic behavior of the entire panel. In order to analyze the behavior, the section shown is simplified as indicated in Figure 2. This simplification replaces the surrounding structure with an equivalent elastic constraint along the edges $x = \pm a/2$. The edges are allowed to rotate but may deflect only in the x-direction. The plate is assumed to be perfectly flat before heating. In addition, heating of the panel is assumed to be uniform over the surface and the temperature a function of z only, i.e., temperature gradients in the x-direction resulting from heat flow into the stringers are neglected.

In general it is recognized that a two-dimensional buckling pattern is possible depending upon the magnitudes of the external loading and the induced loading due to heating. If attention is given only to that portion of the panel far from the ribs it appears possible to neglect curvature in the y-direction. This single curvature assumption essentially views the plate as a wide column.

With the above simplifications, equations (35) and (36) reduce to

$$\nabla^4 \phi = 0 \qquad (37)$$

and

$$\frac{d^4 w}{dx^4} - \frac{N_x}{D_2} \frac{d^2 w}{dx^2} = 0 \qquad (38)$$

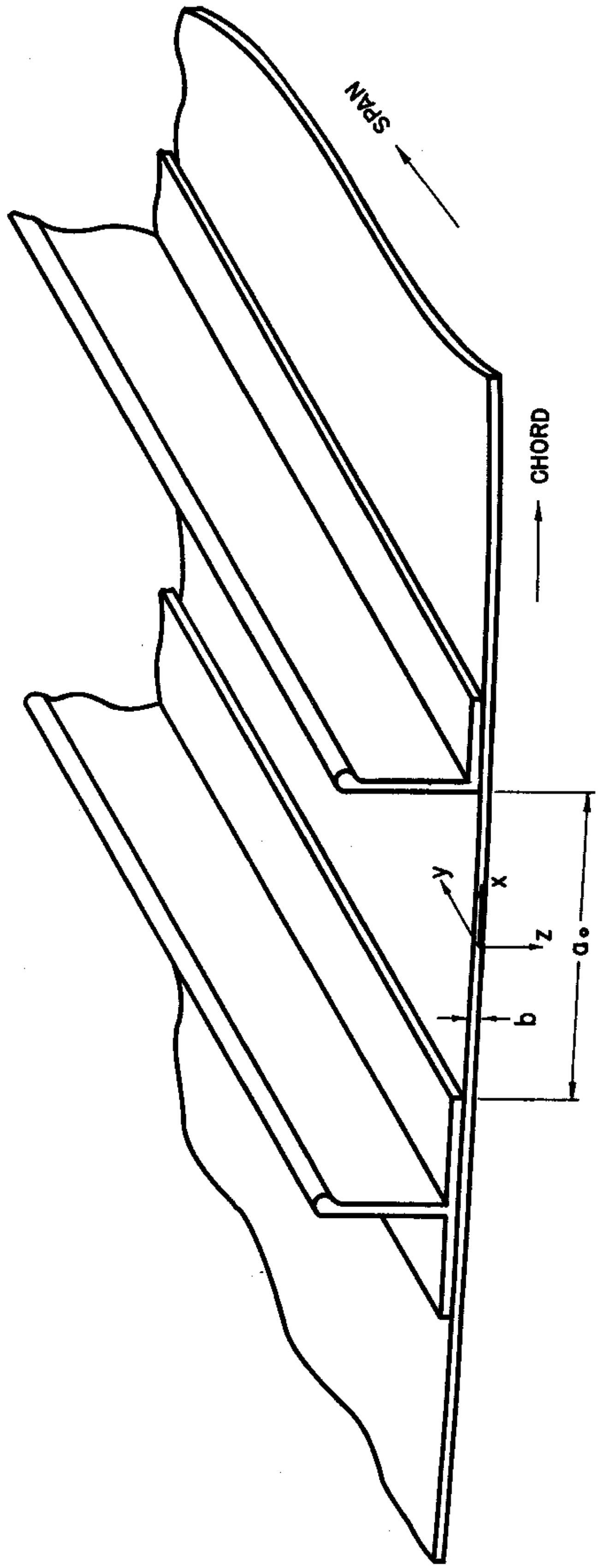

FIGURE I SECTION OF A TYPICAL SHEET-STRINGER PANEL

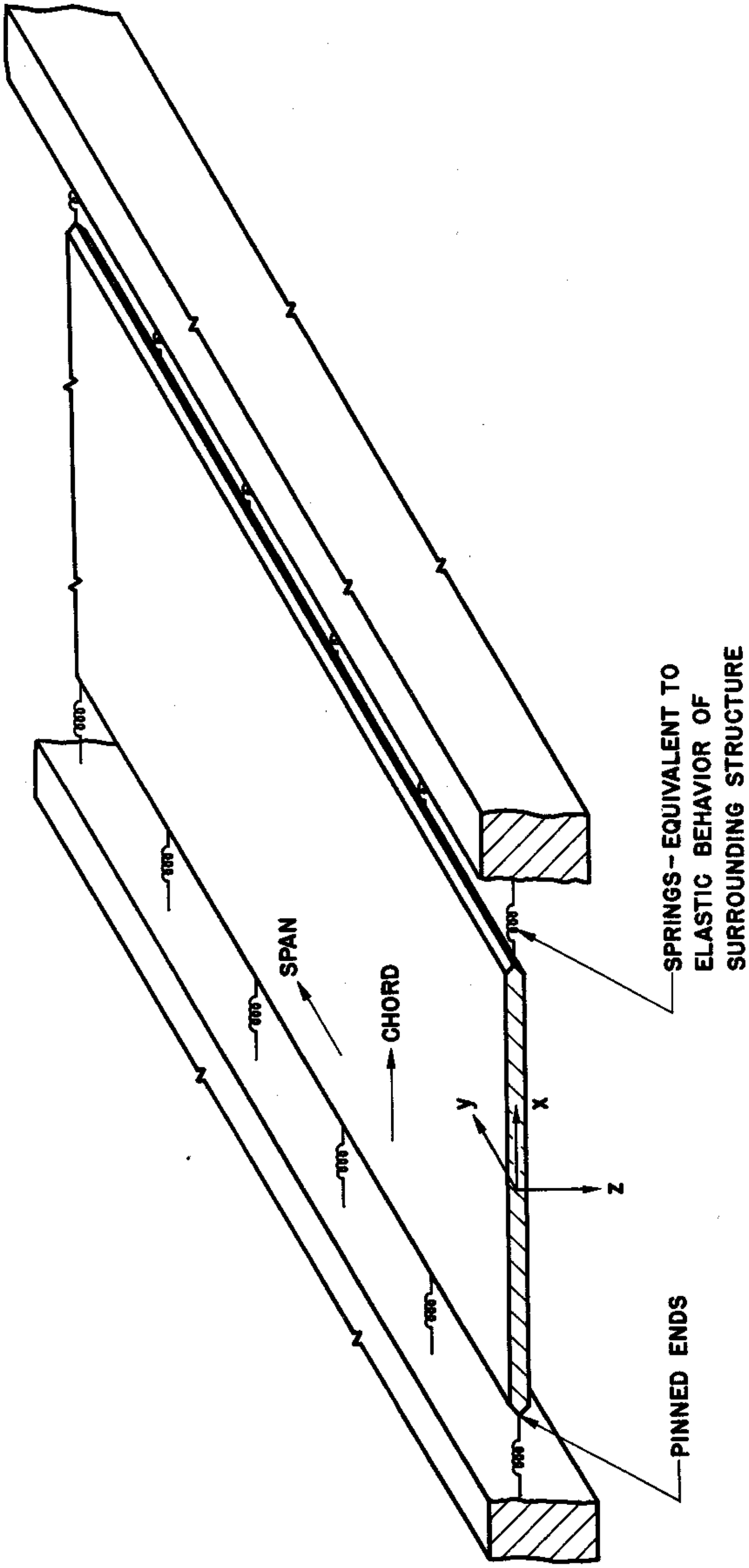

FIGURE 2 SIMPLIFIED COMPONENT OF SHEET-STRINGER PANEL

Equilibrium in the x-direction requires that N_x be a **constant** compressive stress.

The boundary conditions are

$$M_x = 0 \quad \text{at} \quad x = \pm \frac{a_h}{2}$$

and

$$w = 0 \quad \text{at} \quad x = \pm \frac{a_h}{2}$$

where a_h is the chord length of the heated plate (Figure 3). Solving equation (38) for the deflection w gives

$$w = \frac{M_T}{N_x} \left(1 - \frac{\cos cx}{\cos \frac{ca_h}{2}} \right) \tag{39}$$

where

$$c^2 = -\frac{N_x}{D_2}$$

Substituting equation (39) into equations (25) and (26)

$$M_x + M_T = M_T \frac{\cos cx}{\cos \frac{ca_h}{2}} \tag{40}$$

and

$$M_y + M_T = \nu M_T \frac{\cos cx}{\cos \frac{ca_h}{2}} \tag{41}$$

Substitution of equation (40) into equation (28), and equation (41) into equation (29), and using the definitions for D_0 and D_2 given by equations

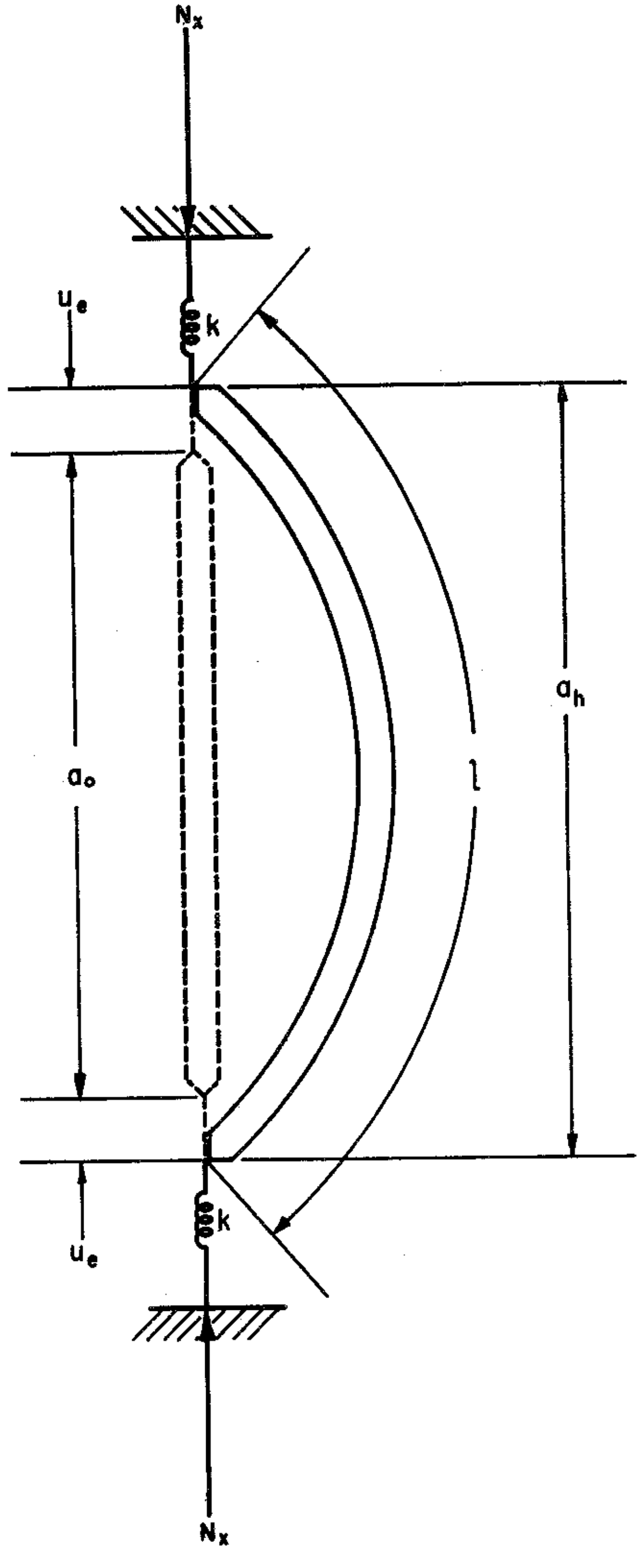

FIGURE 3 HEATED SIMPLIFIED MODEL

(17) and (19) yields the local stresses

$$\sigma_x = (N_x + N_T)\frac{1}{b} + \frac{12M_T}{b^3}\frac{\cos cx}{\cos\frac{ca_h}{2}}z - \frac{E\alpha T}{1-\nu} \tag{42}$$

and

$$\sigma_y = (N_y + N_T)\frac{1}{b} + \frac{12\nu M_T}{b^3}\frac{\cos cx}{\cos\frac{ca_h}{2}}z - \frac{E\alpha T}{1-\nu} \tag{43}$$

The forces N_x and N_y must be found by consideration of all the deformations of the plate. Solving equations (5) and (6) for the strains ϵ_x and ϵ_y and integrating over the thickness of the plate the average strains $\overline{\epsilon}_x$ and $\overline{\epsilon}_y$ are found as functions of the sectional forces N_x and N_y.

$$\overline{\epsilon}_x = \frac{1}{Eb}\left[N_x - \nu N_y + (1-\nu) N_T\right] \tag{44}$$

and

$$\overline{\epsilon}_y = \frac{1}{Eb}\left[N_y - \nu N_x + (1-\nu) N_T\right] \tag{45}$$

The condition of infinite width requires that

$$\overline{\epsilon}_y = 0 \tag{46}$$

Thus,

$$N_y + N_T = \nu(N_x + N_T) \tag{47}$$

Therefore equation (43) becomes

$$\sigma_y = \nu(N_x + N_T)\frac{1}{b} + \frac{12\nu M_T}{b^3}\frac{\cos cx}{\cos\frac{ca_h}{2}}z - \frac{E\alpha T}{1-\nu} \tag{48}$$

Comparing equations (42) and (48), σ_y may be written

$$\sigma_y = \nu\sigma_x - E\alpha T \tag{49}$$

The change of length of the deformed plate (Figure 3) is

$$\delta = l - a_0$$

where l is the length of the curved plate and a_0 is its initial length.

The average strain in the x-direction is then

$$\bar{\epsilon}_x = \frac{\delta}{a_0} = \frac{l}{a_0} - 1 \tag{50}$$

The length l of the deflected plate is found by integrating the transverse deflection curve over the arc length as follows:

$$l = \int_{-a_h/2}^{a_h/2}\left[1 + \left(\frac{dw}{dx}\right)^2\right]^{1/2} dx \tag{51}$$

The length a_h may be given in terms of the initial length a_0 and the displacement at the ends of the plate by the expression

$$a_h = a_0 + 2u_e \tag{52}$$

Since the slope dw/dx is always small compared to unity, the integrand of equation (51) may be approximated by the first two terms of its binomial expansion. Thus,

$$l \cong \int_{-(a_0/2 + u_e)}^{(a_0/2 + u_e)} \left[1 + \frac{1}{2} \left(\frac{dw}{dx}\right)^2\right] dx \tag{53}$$

The slope dw/dx is determined from the transverse deflection equation (39).

$$\frac{dw}{dx} = \frac{cM_T}{N_x} \frac{\sin cx}{\cos \frac{cd_h}{2}} \tag{54}$$

Substituting equation (54) in equation (53) and integrating, the deflected length is given as

$$l = a_0 + 2u_e + \frac{1}{2}\left(\frac{cM_T}{N_x}\right)^2 \left[\frac{a_0 + 2u_e - \frac{1}{c} \sin c\,(a_0 + 2u_e)}{1 + \cos c\,(a_0 + 2u_e)}\right] \tag{55}$$

If the constraint responds elastically to the inplane force N_x as a spring of stiffness K per unit length of plate edge, then

$$N_x = -Ku_e \tag{56}$$

The negative sign indicates that the compressive load N_x is associated with an elongation u_e at each end of the plate. Eliminating u_e from equation (55)

$$l = a_0 - \frac{2N_x}{a_0 K} + \frac{1}{2}\left(\frac{cM_T}{N_x}\right)^2 \left[\frac{a_0 - \frac{2N_x}{K} - \frac{1}{c} \sin c\left(a_0 - \frac{2N_x}{K}\right)}{1 + \cos c\left(a_0 - \frac{2N_x}{K}\right)}\right] \tag{57}$$

This may now be substituted in equation (50) to give

$$\bar{\epsilon}_x = -\frac{2N_x}{K} + \frac{1}{2}\left(\frac{cM_T}{N_x}\right)^2 \left[\frac{1 - \frac{2N_x}{a_0 K} - \frac{1}{ca_0} \sin c\left(a_0 - \frac{2N_x}{K}\right)}{1 + \cos c\left(a_0 - \frac{2N_x}{K}\right)}\right] \qquad (58)$$

The simultaneous solution of equations (44), (45) and (58) results in the following relation between N_T and N_x.

$$N_T = -\left[1 + \frac{Eb}{1 - \nu^2}\,\theta\right] N_x - 6\,\frac{M_T^2}{b^2 N_x}\left[\frac{1 - \theta N_x - \frac{1}{ca_0} \sin ca_0(1-\theta N_x)}{1 + \cos ca_0(1 - \theta N_x)}\right] \qquad (59)$$

where

$$\theta = \frac{2}{a_0 K} \qquad (60)$$

Because equation (59) is transcendental, a graphical method was used to obtain N_x in terms of N_T and M_T. This relation now allows the determination of local stresses (Eqs. (42) and (49)) and deflections (Eq. (39)).

3. Limiting Conditions for the In-Plane Forces

Equation (59) establishes some very significant restrictions on the in-plane force N_x. It is seen that for any finite value of N_T the denominator of the last term of equation (59) must not vanish. This results in the condition

$$ca_0\,(1 - \theta\,N_x) < \pi \qquad (61)$$

For the case of rigid constraints ($\theta = 0$) equation (61) reduces to

$$ca_0 = a_0 \sqrt{-\frac{N_x^*}{D_2}} < \pi \qquad (62)$$

If the temperature variation across the thickness of the plate is small, the variation of Young's Modulus E across the thickness of the plate will also be small and D_2 may be written

$$D_2 = \frac{Eb^3}{12(1 - \nu^2)} \qquad (63)$$

Thus, the limiting value $N^*_{x_{cr}}$ of the in-plane force N_x is

$$N^*_{x_{cr}} = -\frac{\pi^2 E b^3}{12(1 - \nu^2)a_0^2} \qquad (64)$$

Multiplying by the width of the plate, the critical load P_{cr} for a plate with moment of inertia I is

$$P_{cr} = -\frac{\pi^2 EI}{(1 - \nu^2)a_0^2} \qquad (65)$$

This definition of the critical load is exactly the same as that given by the Euler formula for the isothermal buckling of flat plates in compression.[6] The distinction between the isothermal and non-isothermal cases is important, however, and should be noted. In the isothermal case an externally applied load on an initially flat plate may be increased until the Euler critical load is reached, at which time the plate buckles and fails if the load is not removed or relieved. In the non-isothermal case the in-plane force N_x increases due to restraint of thermal expansion as the temperature (and N_T) is increased. The increase in N_T is generally accompanied by some thermal moment. As the plate departs from flatness the force N_x is relieved. Thus the critical value $N^*_{x_{cr}}$ is not reached. Increasing N_T further results in greater transverse deflections while the in-plane force N_x asymptotically approaches the critical value $N^*_{x_{cr}}$. This asymptotic behavior is illustrated in Figure 7..

Again, for the case of rigid constraints ($\theta = 0$), we find by inspection of equation (59) that when the thermal moment M_T is zero, $N_x = -N_T$, until the critical value is reached at which time equation (59) is indeterminate.

For any finite value of K (elastic constraints) equation (61) results in a cubic in $N_{x_{cr}}$

$$\theta^2 N_{x_{cr}}^3 - 2\,\theta N_{x_{cr}}^2 + N_{x_{cr}} = -\frac{\pi^2 E b^3}{12(1-\nu^2)a_0^2} = N_{x_{cr}}^* \tag{66}$$

Dividing by $N_{x_{cr}}$ and factoring out $N_{x_{cr}}$

$$\theta N_{x_{cr}}\left[\theta N_{x_{cr}} - 2\right] + 1 = \frac{N_{x_{cr}}^*}{N_{x_{cr}}}$$

It can be shown that $\theta N_{x_{cr}}$ must be less than αT. Therefore, $\theta N_{x_{cr}}$ may be considered small compared to 2 and is dropped from the term in parentheses. The resulting equation is a quadratic in $N_{x_{cr}}$, the solution of which is

$$N_{x_{cr}} = 2N_{x_{cr}}^*\left[\frac{1}{1 + \sqrt{1 - 8\theta N_{x_{cr}}^*}}\right] \tag{67}$$

The effect of θ is two-fold. Increasing θ lowers the limiting value of N_x and also reduces the slope of the boundary curve described by

$$N_y = -\left[1 + \frac{E b}{1-\nu}\theta\right] N_x \tag{68}$$

4. Dimensionless Relations

The above method of solution is effected most advantangeously by writing the significant equations in terms of dimensionless groups. The following dimensionless parameters are employed:

$$z^+ \equiv \frac{z}{b}, \quad w^+ \equiv \frac{w}{b}, \quad x^+ \equiv \frac{x}{a_0}, \quad a_0^+ \equiv \frac{a_0}{b} \tag{69}$$

$$N_T^+ \equiv \frac{(1-\nu)N_T}{E\alpha T_{ref}\, b}, \quad N_x^+ \equiv \frac{(1-\nu)N_x}{E\alpha T_{ref}\, b} \tag{70}$$

$$M_T^+ \equiv \frac{(1-\nu)M_T}{E\alpha T_{ref}\, b^2}, \quad M_x^+ \equiv \frac{(1-\nu)M_x}{E\alpha T_{ref}\, b^2} \tag{71}$$

$$T^+ \equiv \frac{T}{T_{ref}} \tag{72}$$

$$\sigma_x^+ \equiv \frac{(1-\nu)\sigma_x}{E\alpha T_{ref}}, \quad \sigma_y^+ \equiv \frac{(1-\nu)\sigma_y}{E\alpha T_{ref}} \tag{73}$$

$$\psi \equiv a_0^+ \left[-12(1+\nu)\,\alpha\, T_{ref} \right]^{1/2} \tag{74}$$

$$\theta^+ \equiv \frac{E\alpha T_{ref}\, b}{1-\nu}\,\theta = \frac{2\, E\alpha T_{ref}\, b}{(1-\nu)a_0\, K} \tag{75}$$

In terms of these dimensionless quantities equations (42), (48), (49) and (39) are written as follows:

$$\sigma_x^+ = N_x^+ + N_T^+ + 12\, M_T^+\, z^+ \frac{\cos \psi\, N_x^{+\frac{1}{2}}\, x^+}{\cos\left[\frac{\psi N_x^{+\frac{1}{2}}}{2}(1 - \theta^+ N_x^+)\right]} - T^+ \tag{76}$$

$$\sigma_y^+ = \nu \left\{ N_x^+ + N_T^+ + 12 M_T^+\, z^+ \frac{\cos \psi\, N_x^{+\frac{1}{2}}\, x^+}{\cos\left[\frac{\psi N_x^{+\frac{1}{2}}}{2}(1 - \theta^+ N_x^+)\right]} \right\} - T^+ \tag{77}$$

or

$$\sigma_y^+ = \nu\, \sigma_x^+ - (1 - \nu)\, T^+ \tag{78}$$

and

$$w^+ = \frac{M_T^+}{N_x^+} \left\{ 1 - \frac{\cos \psi\, N_x^{+\frac{1}{2}}\, x^+}{\cos\left[\frac{\psi N_x^{+\frac{1}{2}}}{2}(1 - \theta^+ N_x^+)\right]} \right\} \tag{79}$$

Equation (59) is written as

$$N_T^+ = -\left(1 + \frac{\theta^+}{(1+\nu)\alpha T_{ref}}\right) N_x^+ - 6\, \frac{M_T^{+2}}{N_x^+} \left\{ \frac{1 - \theta^+ N_x^+ - \frac{1}{\psi N^{+\frac{1}{2}}} \sin\left[\psi N_x^{+\frac{1}{2}}\,(1 - \theta^+ N_x^+)\right]}{1 + \cos\left[\psi N_x^{+\frac{1}{2}}(1 - \theta^+\, N_x^+\,)\right]} \right\} \tag{80}$$

For the rigid constraint case ($\theta^{+}= 0$) equation (80) reduces to

$$N_T^{+} = -N_x^{+} - 6\,\frac{M_T^{+}}{N_x^{+}}\left[\frac{1+\dfrac{1}{\psi N_x^{+1/2}}\sin\psi\, N_x^{+1/2}}{1+\cos\psi\, N_x^{+1/2}}\right] \tag{81}$$

The dimensionless critical load is given by

$$N_{x_{cr}}^{+} = 2\,N_{x_{cr}}^{*+}\left(\frac{1}{1+\sqrt{1-8N_{x_{cr}}^{*+}\,\theta^{+}}}\right) \tag{82}$$

where

$$N_{x_{cr}}^{*+} = -\frac{\pi^2}{12(1+\nu)\alpha\, T_{ref}\, a_0^{+2}} = \left(\frac{\pi}{\psi}\right)^2 \tag{83}$$

is the dimensionless critical load for the rigid constraint case.

SECTION II
COMBINED HEAT TRANSFER AND HEATED PLATE STRESS ANALYSIS

1. Elastic Response to Heat Input Function

The above thermo-elastic analysis requires a knowledge of the thermal force (N_T) and thermal moment (M_T) for each temperature distribution. Naturally, the transient thermal response must be obtained from solutions to the heat conduction equation for the particular heat input function and thermal boundary conditions of interest. The thermal response of a system consisting of a flat plate irradiated and cooled on one side and insulated on the other side (see Figure 4) was used to analytically evaluate the thermal force and moment. These results, reported in reference 3, were used along with equations (76), (79), and (80) for the evaluation of the transient response of the stresses and deflections for the rigid constraint case ($\theta = 0$).

2. Sample Calculation of Stresses and Deflections

To illustrate the method by which the stresses and deflections are obtained a sample calculation is shown below. The constants of the system for which the sample calculation was made are:

$\rho_0 = 173$ lb/ft^3

$C_p = 0.23$ Btu/lb °F

$k = 66.7$ Btu/hr ft °F

$E\alpha = 130$ psi/°F

$\nu = 0.33$

$a_0 = 5.75$ in.

$b = 3/16$ in.

$Q = 44$ Btu/ft^2

$h_c = 42$ Btu/hr ft^2 °F

$\eta = 8.35 \times 10^{-4}$ hr

$$Bi = \frac{h_c b}{k} = 0.01$$

$$\beta = \frac{b}{\sqrt{a\eta}} = 0.4$$

$$T_{ref} = \frac{Q}{\rho C_p b} = 71.2 \text{ °F}$$

$\psi = 3.36$

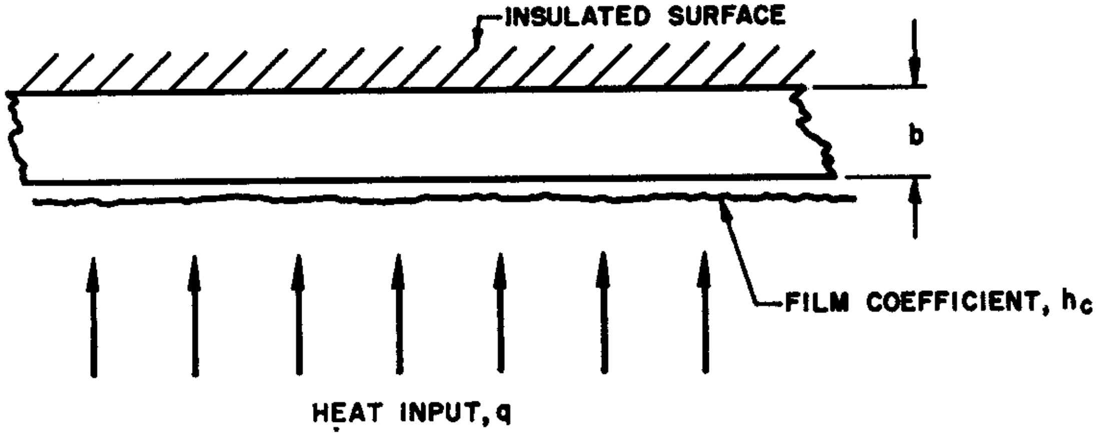

HEAT TRANSFER SYSTEM

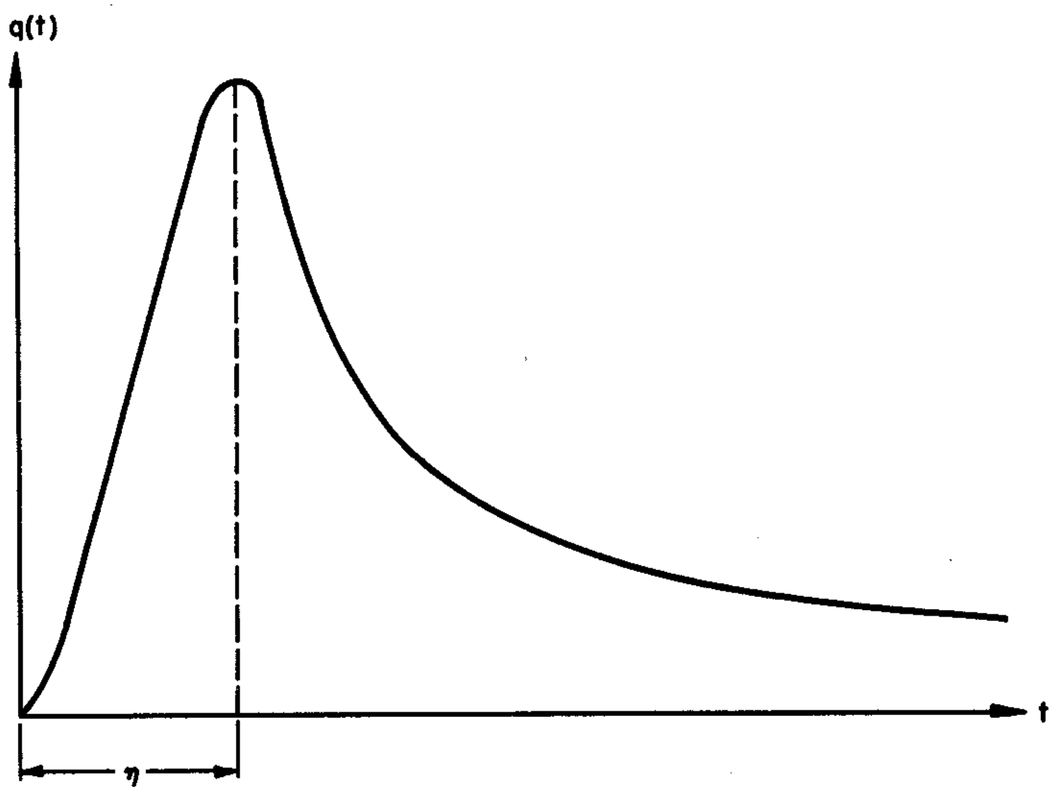

HEAT INPUT FUNCTION

FIGURE 4 IDEALIZED HEAT TRANSFER SYSTEM AND HEAT INPUT FUNCTION

Using the above values of Biot's Modulus and β, the appropriate thermal force, thermal moment and temperature histories were chosen from reference 3. These curves are shown in Figures 5 and 6.

Prior to evaluation of the stresses and deflections equation (81) was plotted (Figure 7) in order to facilitate the determination of N_x^+. Entering Figure 7 with the values of N_T^+ and M_T^+ taken from Figures 5 and 6 the corresponding values of N_x^+ were found and inserted in equations (76) and (79). This procedure gave the stresses and deflections at each time t^+. The stresses and deflections for the sample calculation are shown in Figures 8 and 10 respectively. Curves for plates of other lengths are also shown. It is seen that only for a_0 = 5.75 in. does the deflection exceed one percent of the thickness. For this plate the maximum deflection is approximately 5% and occurs as N_x^+ approaches its critical value. The initial deflection at $t^+ = 1$ is primarily due to the influence of the moment, M_T^+, while the peak deflection at $t^+ = 6$ is due to the force N_x^+. For the two shorter plates, a_0 = 5.00, 5.50 in., the stresses on the two surfaces do not differ greatly. This is due to the fact that a very slight amount of transverse deflection (bending) occurs in these plates. For the longest plate (a_0 = 5.75 in.) the front and back surface stresses are significantly different since a much larger deflection occurs.

The effect of varying the thickness is shown in Figures 9 and 11. The behavior of the idealized system is highly sensitive to changes in thickness since this alters the heat transfer system as well as the structural system. Calculations were made for a 5.5 in. plate length with thicknesses of 0.125 in., 0.187 in. and 0.250 in. For the two thicker plates the transverse deflection was never greater than one percent of the thickness. Because the amount of bending was so slight the stresses on the heated and insulated surfaces were almost the same. The maximum transverse deflection for the thinnest plate (0.125 in) is 84% of the thickness. This larger deflection caused a complete stress reversal to occur giving tension on the heated face and compression on the insulated face.

It should be noted that the plate was assumed to be initially flat. Although it is known that the effect of initial eccentricity is to lower the critical load, it is not clear just how this variable would affect this analysis. However, the thermal moment appears to play the same role as the initial eccentricity in the isothermal case. That is, the moment causes an early bifurcation of the extreme fiber stresses in the same manner as explained in reference 7.

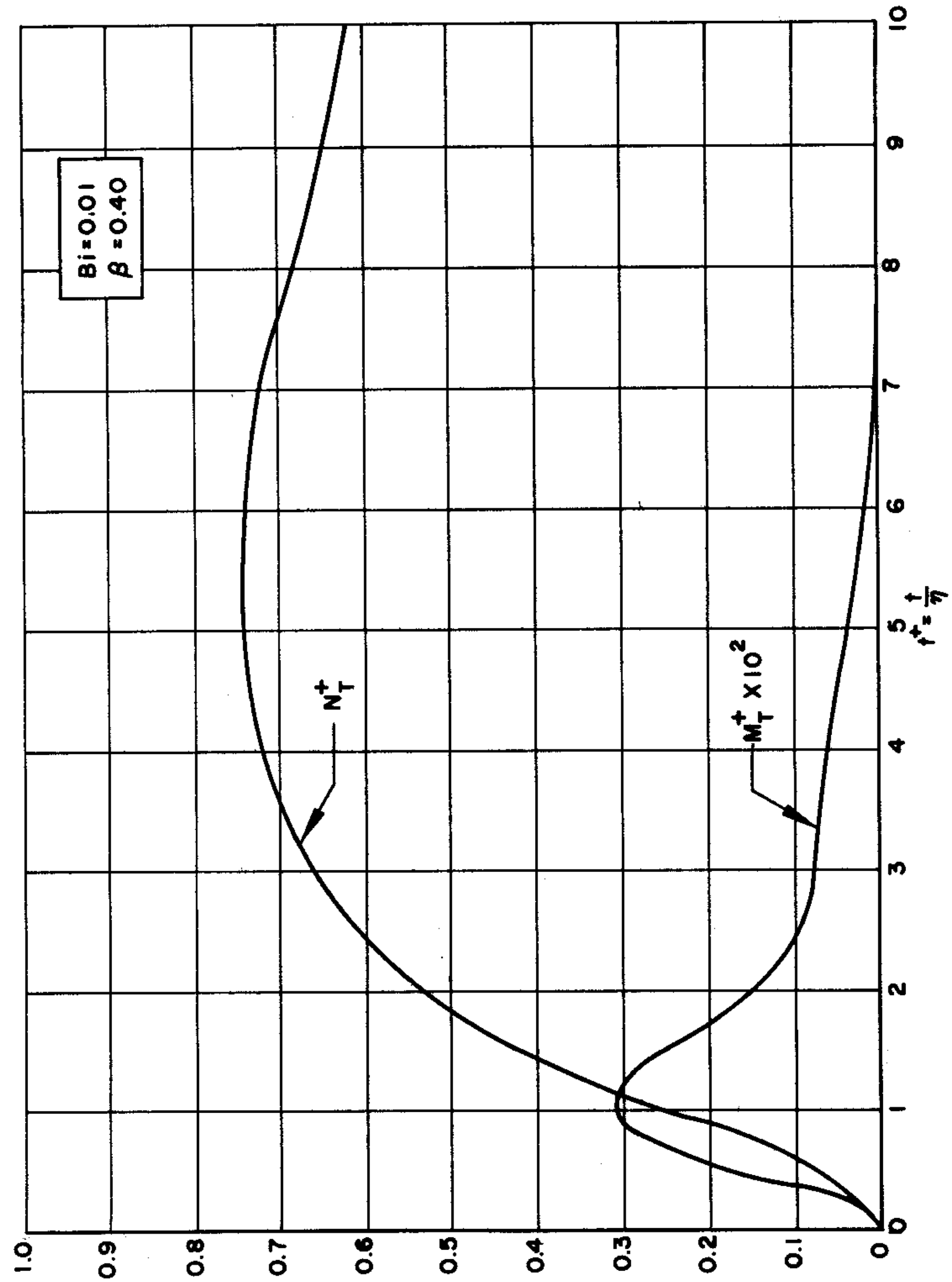

FIGURE 5 THERMAL FORCE AND THERMAL MOMENT

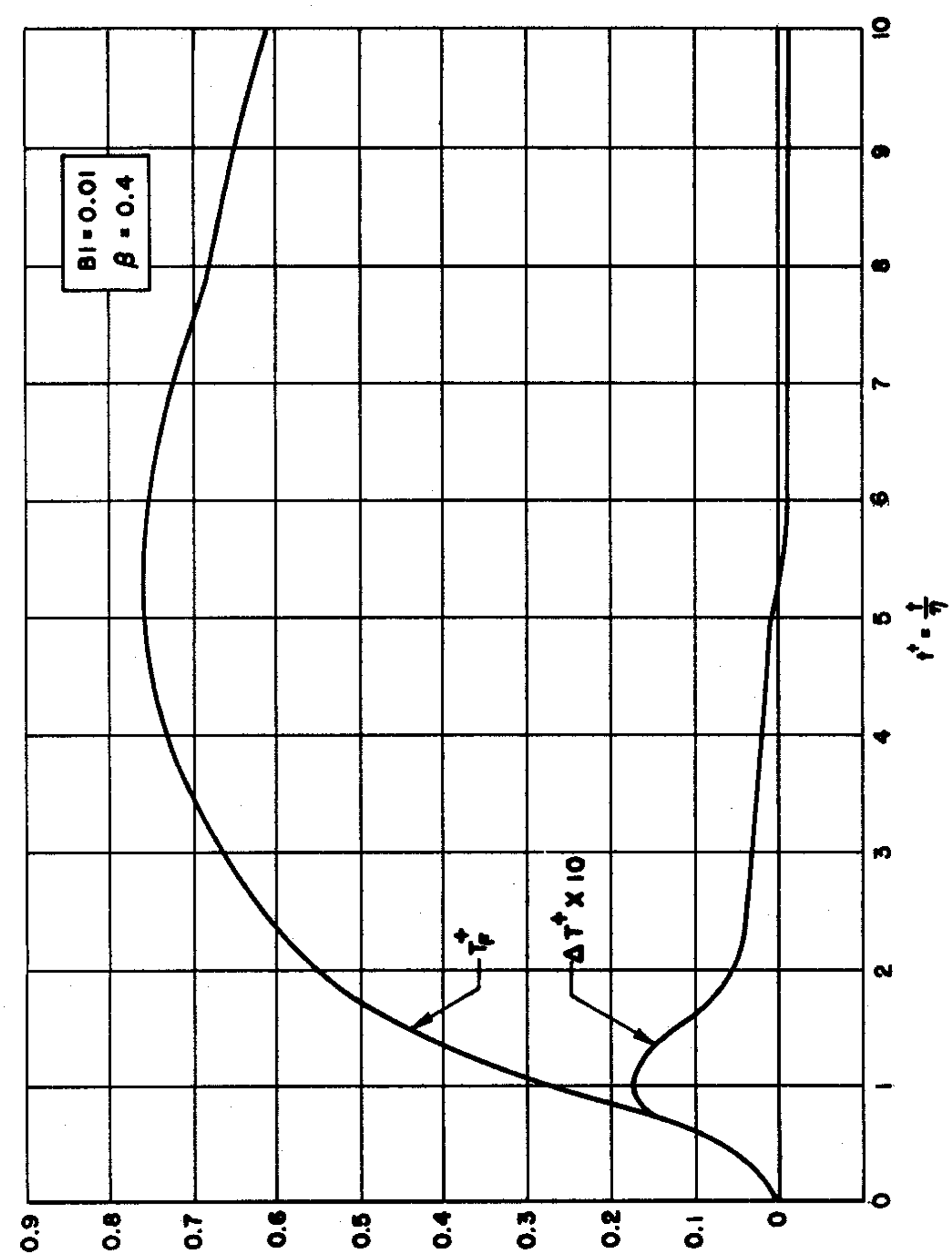

FIGURE 6 FRONT SURFACE TEMPERATURE AND TEMPERATURE DIFFERENCE

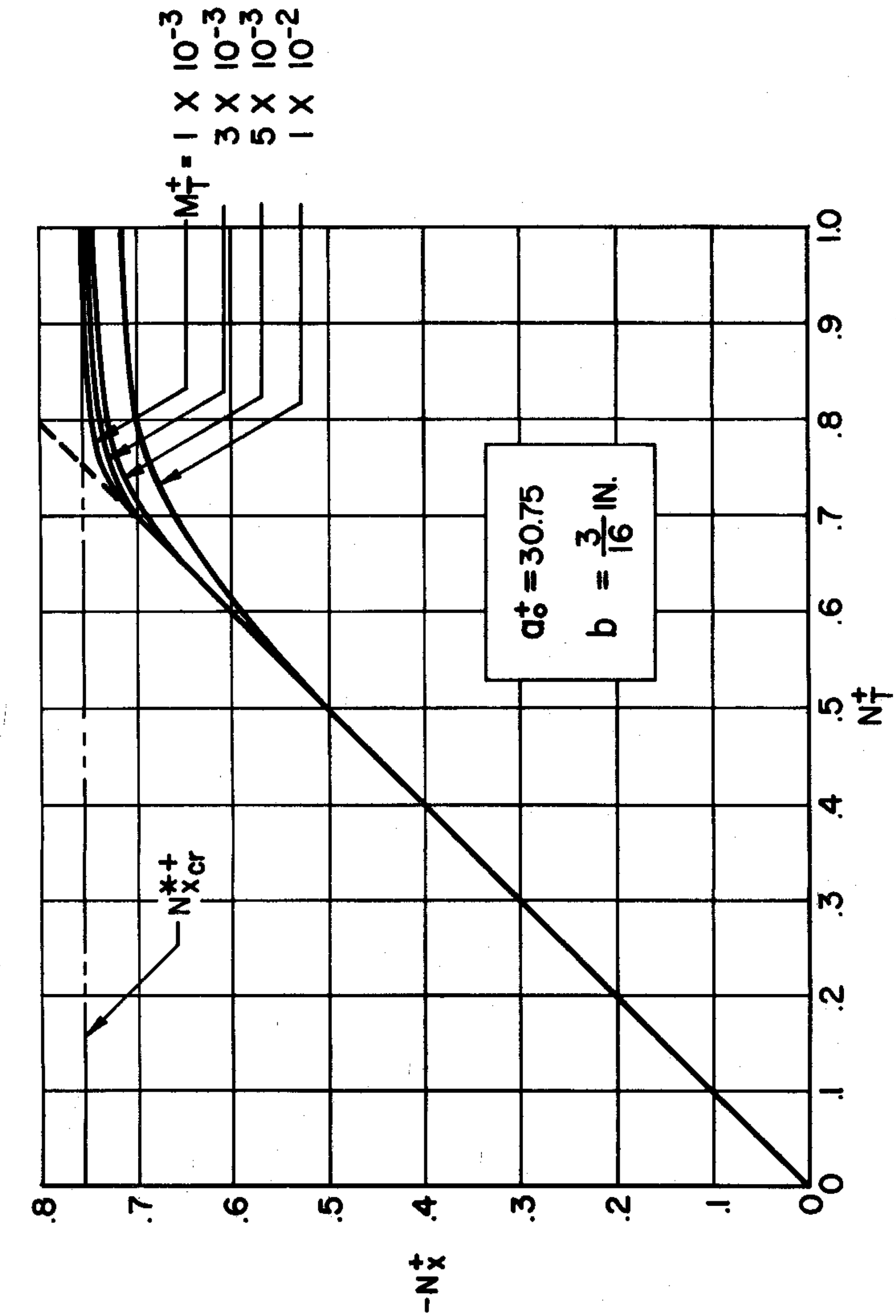

FIGURE 7 IN-PLANE FORCE (N_x^+) VS THERMAL FORCE (N_T^+)

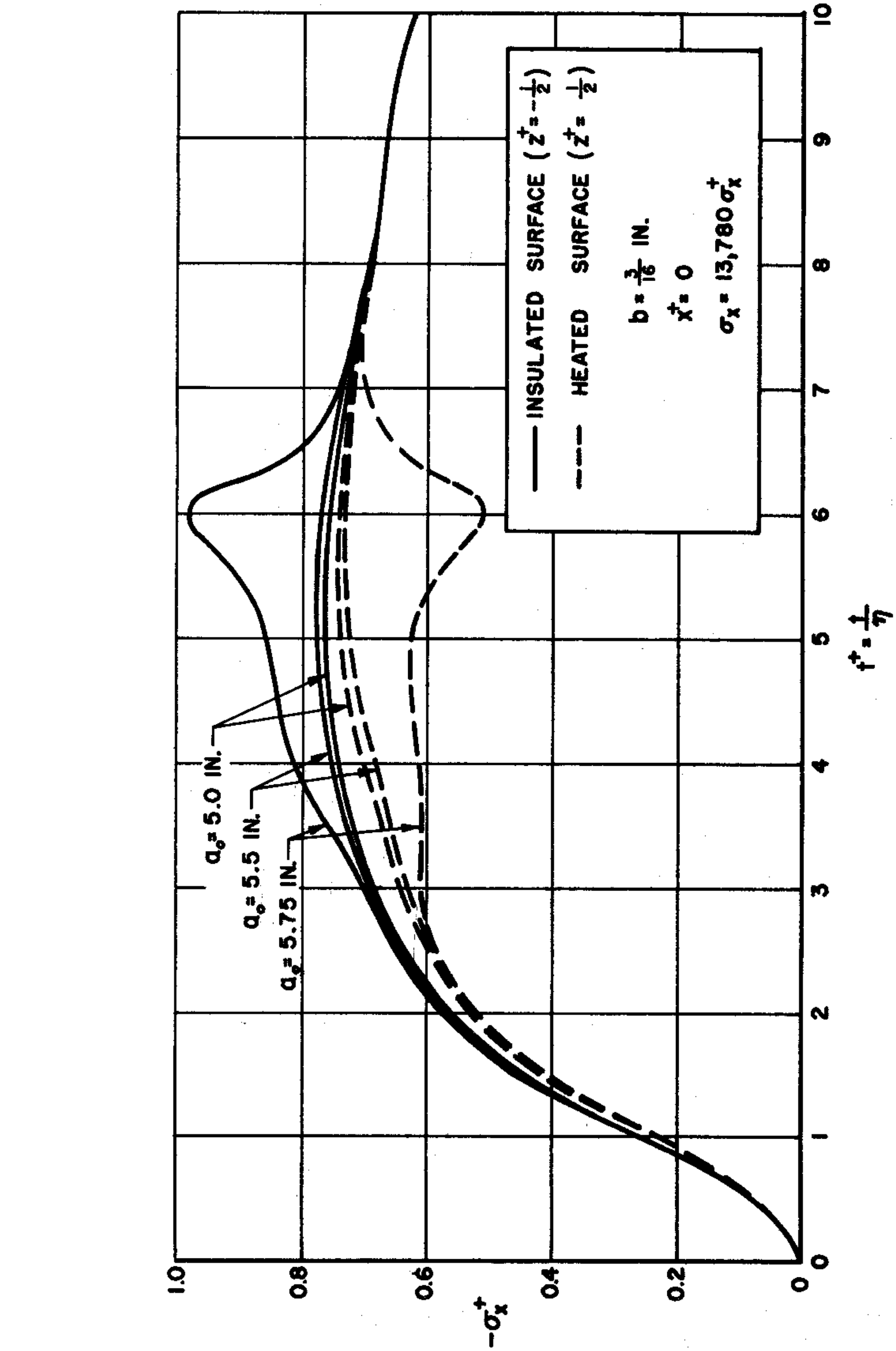

FIGURE 8 SURFACE STRESSES FOR PLATES OF DIFFERENT LENGTHS

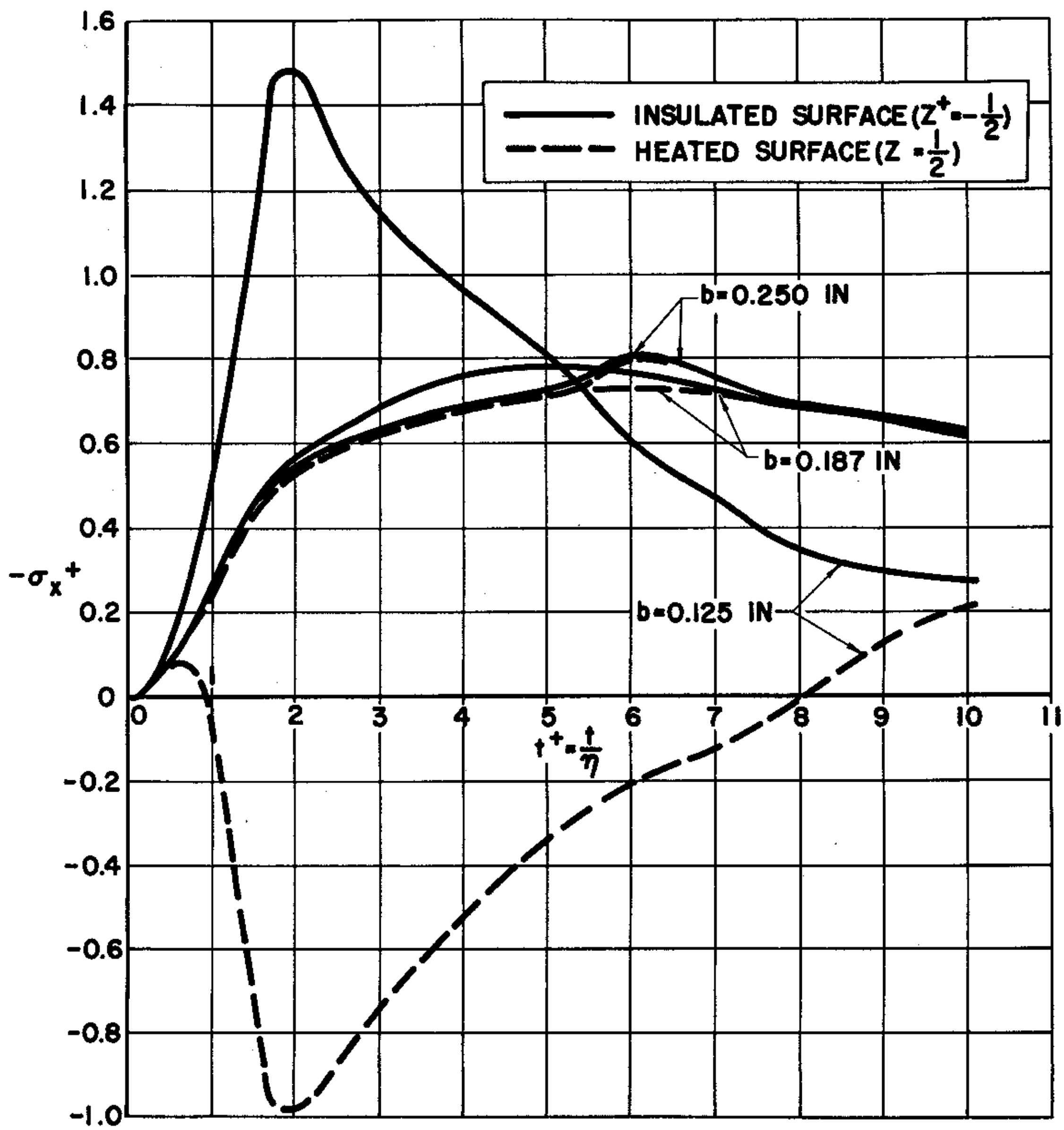

FIGURE 9 SURFACE STRESSES FOR PLATES OF DIFFERENT THICKNESSES (a_o=5.5 IN.)

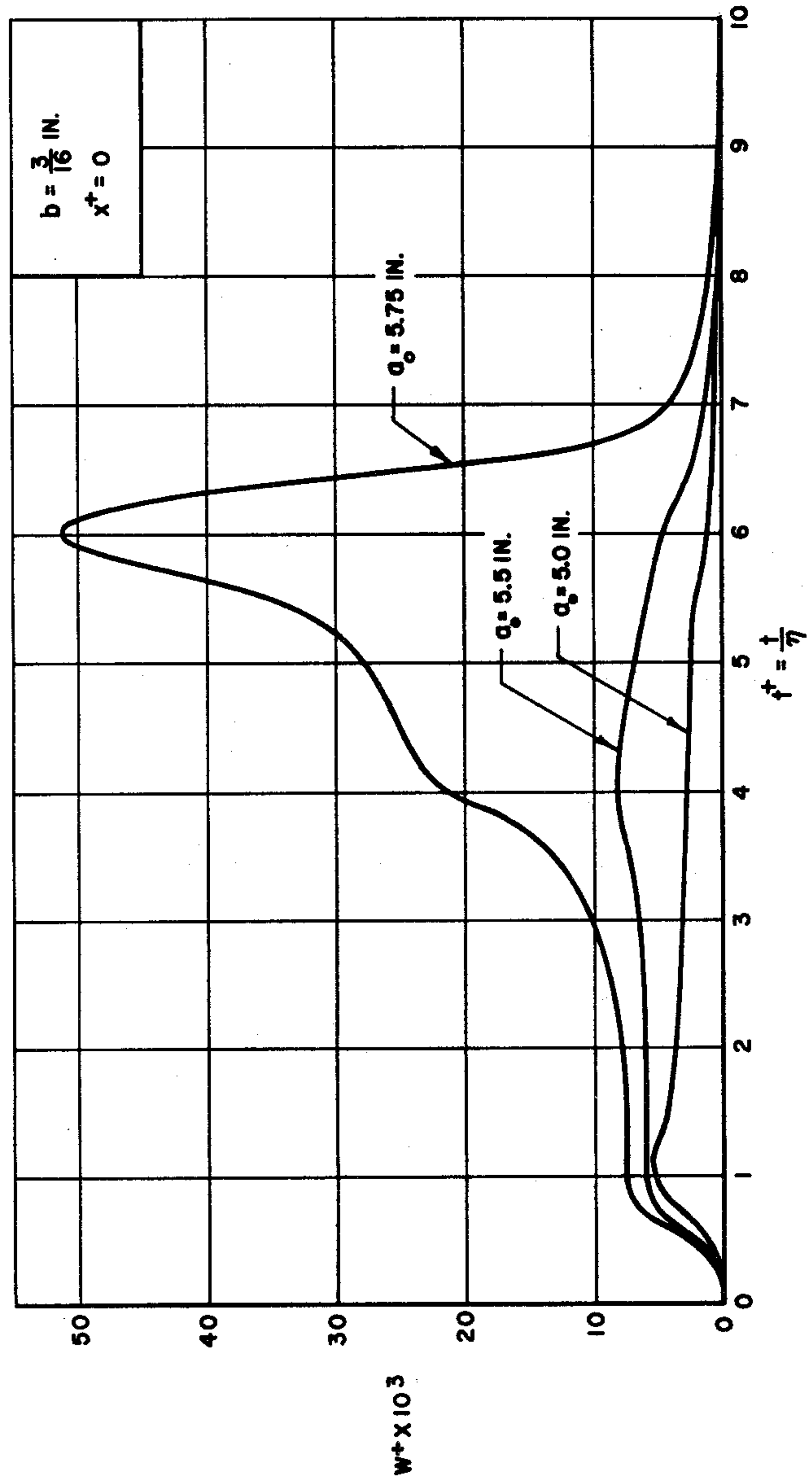

FIGURE 10 TRANSVERSE DEFLECTIONS FOR PLATES OF DIFFERENT LENGTHS

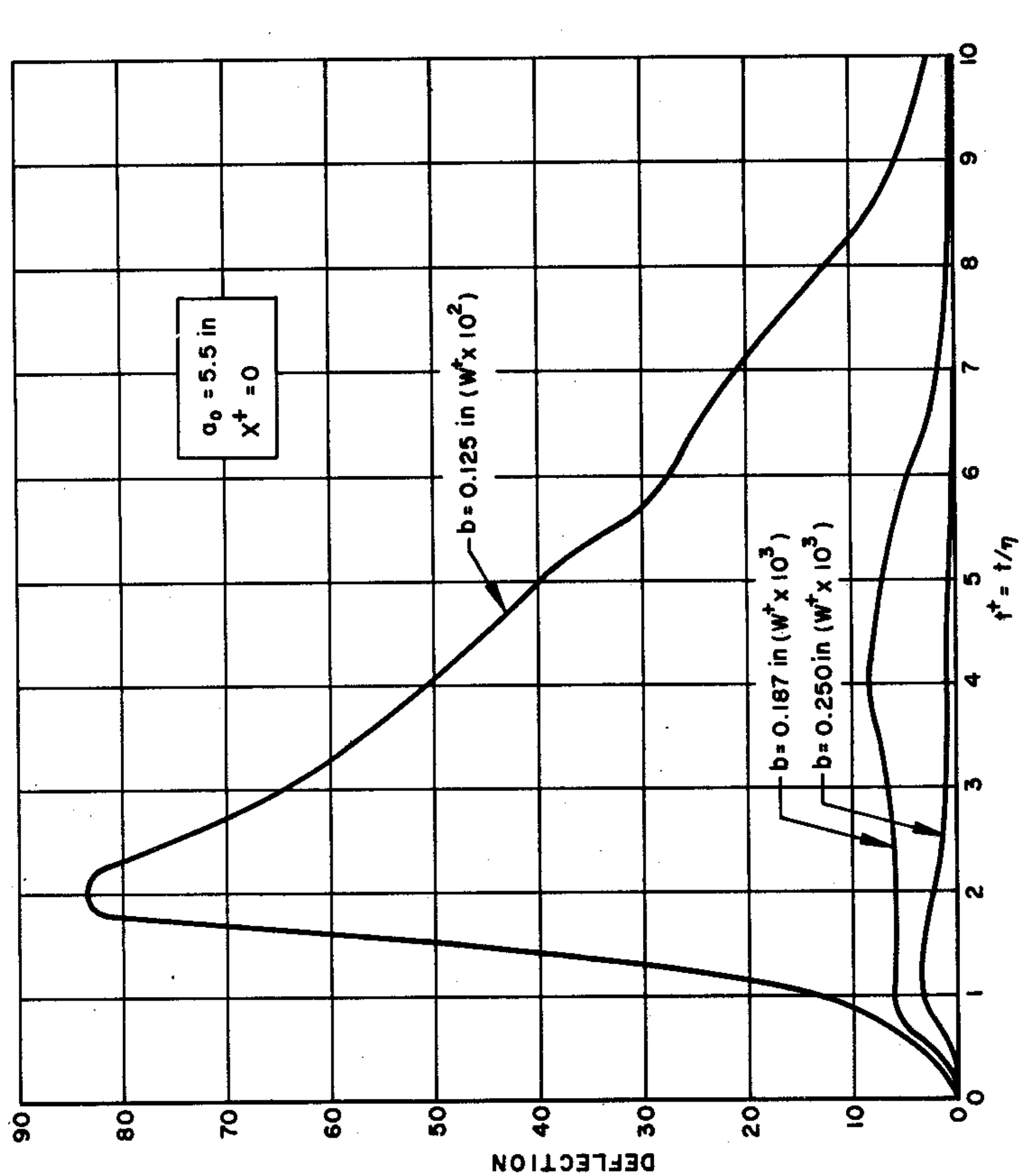

FIGURE 11 TRANSVERSE DEFLECTIONS FOR PLATES OF DIFFERENT THICKNESSES

2. Survey Experiment

In order to experimentally verify the above results a survey experiment was conducted with aluminum plates measuring 4 inches by 8 inches and with thicknesses varying from 1/16 inch to 3/8 inch in the different plates. The plates were blackened on one side and irradiated with a number of heat lamps. The specimens were held between the loading heads of a Baldwin testing machine and the load manually controlled so that the 4 inch length remained approximately ($\pm$ 0.001 in.) constant during the heating. The compressive load on the plate was read directly from the testing machine dial. The experimental configuration is shown schematically in Figure 12.

Typical results are shown in Figure 13 in which the temperature and load response are shown for a plate in which the ratio of length (4 in.) to thickness is 29.5. It was observed that when the plate is constrained and sufficiently heated a curve such as that shown in Figure 14 is obtained. The results for plates of two other thicknesses are also shown.

Figure 14 indicates that after the maximum load was reached the decrease in load exerted by the plate on the testing machine head was greater for the thicker plates. This behavior is attributed to the fact that, although all of the plates deformed inelastically, the inelastic deformation was greater in the thicker plates. The behavior of the thinner plate ($a/b = 47.0$) more closely corresponded to the behavior predicated by equations (59) and (65), although equation (65) gives a value of the critical load which is about 16% lower than the maximum load indicated in Figure 14 (for a/b = 47.0). For the thicker plates the discrepancy is larger. The temperatures at maximum load were somewhat higher than those predicted by the elastic analysis for the rigid constraint case. This is attributed to the fact that the plates were not perfectly constrained. The need for more controlled experiments is evident.

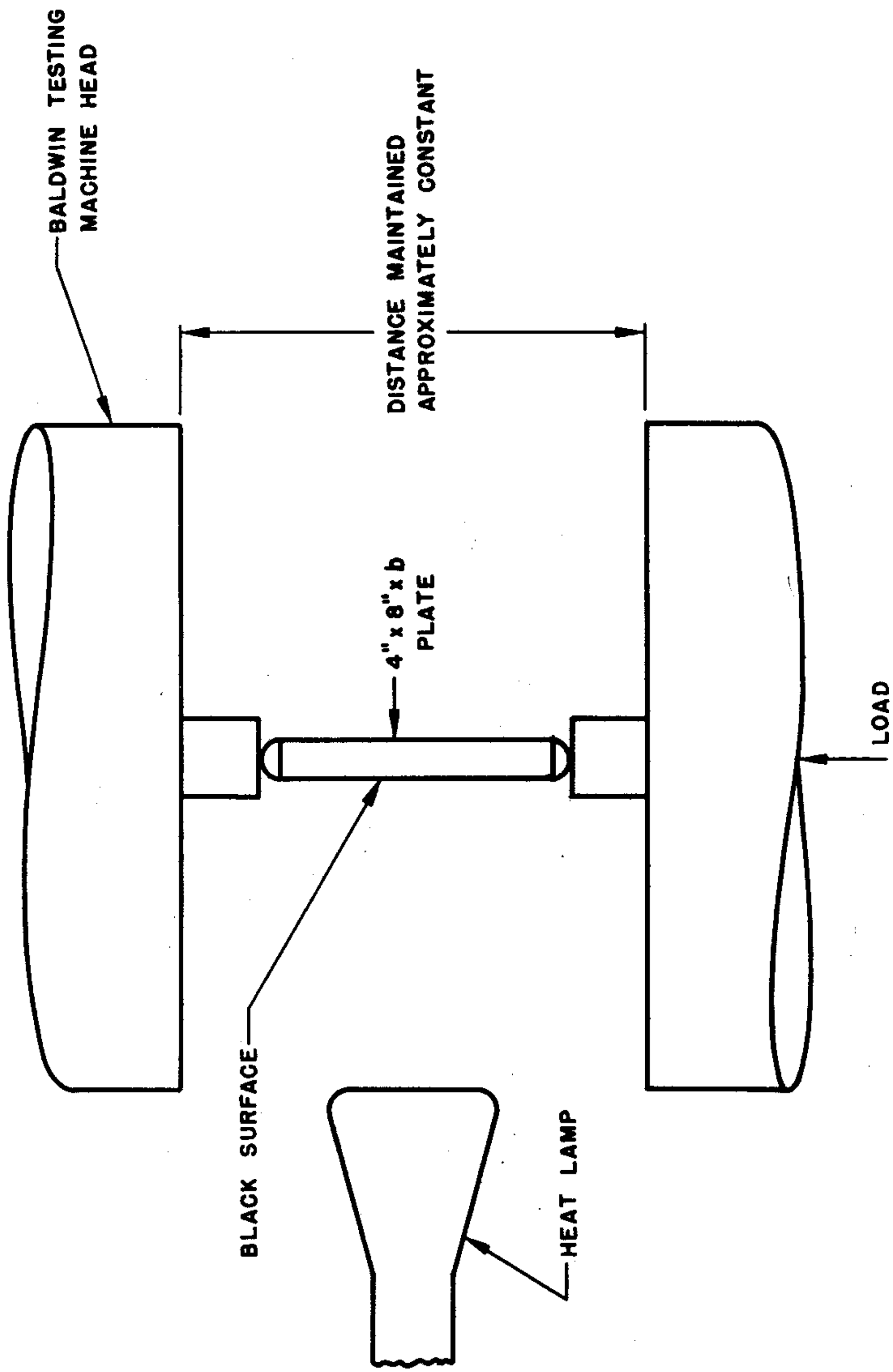

FIGURE 12 SURVEY EXPERIMENT: RADIANTLY HEATED PLATE

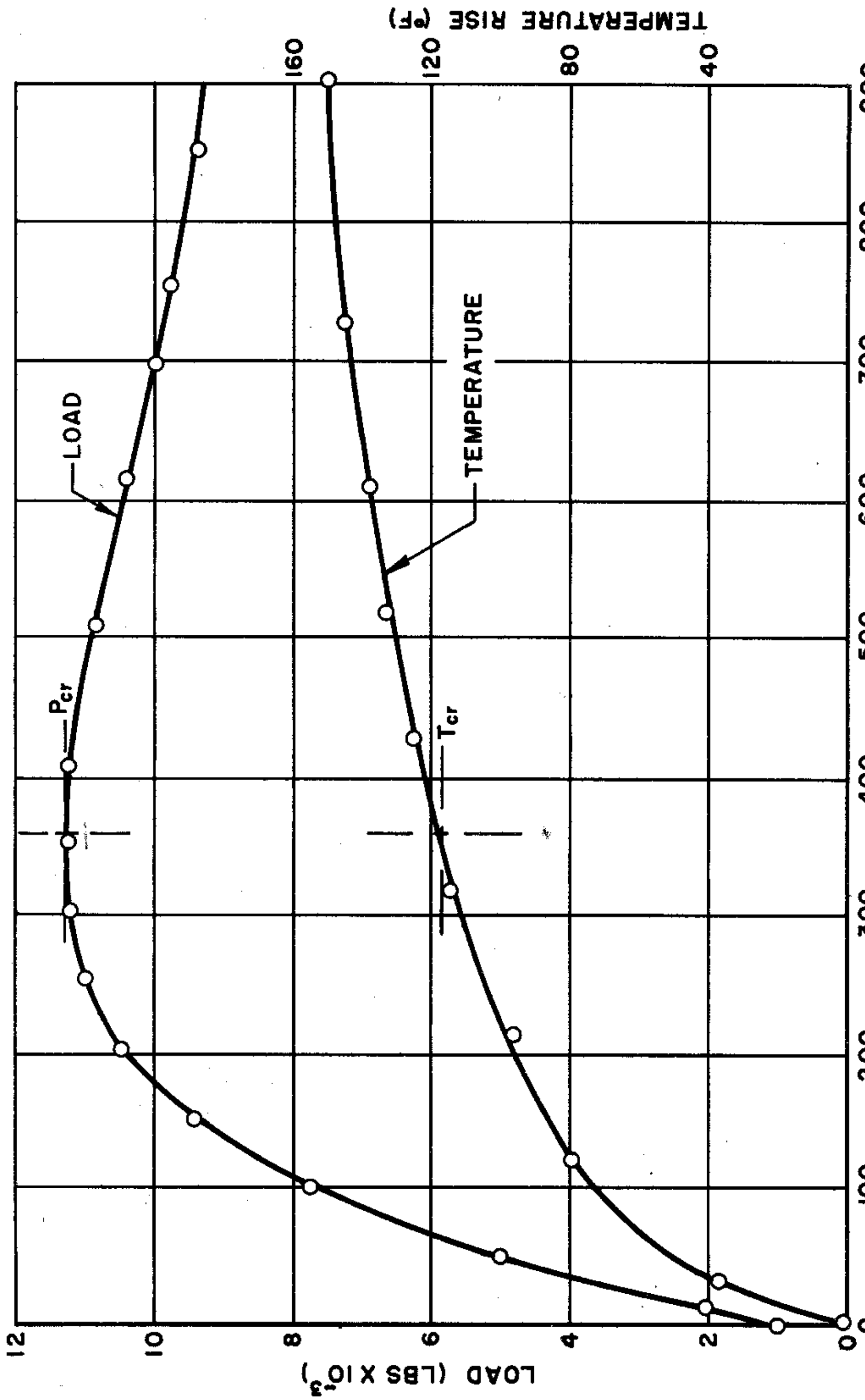

FIGURE 13 SURVEY EXPERIMENT: TYPICAL LOAD AND TEMPERATURE CURVES VS TIME (a_o/b=29.5)

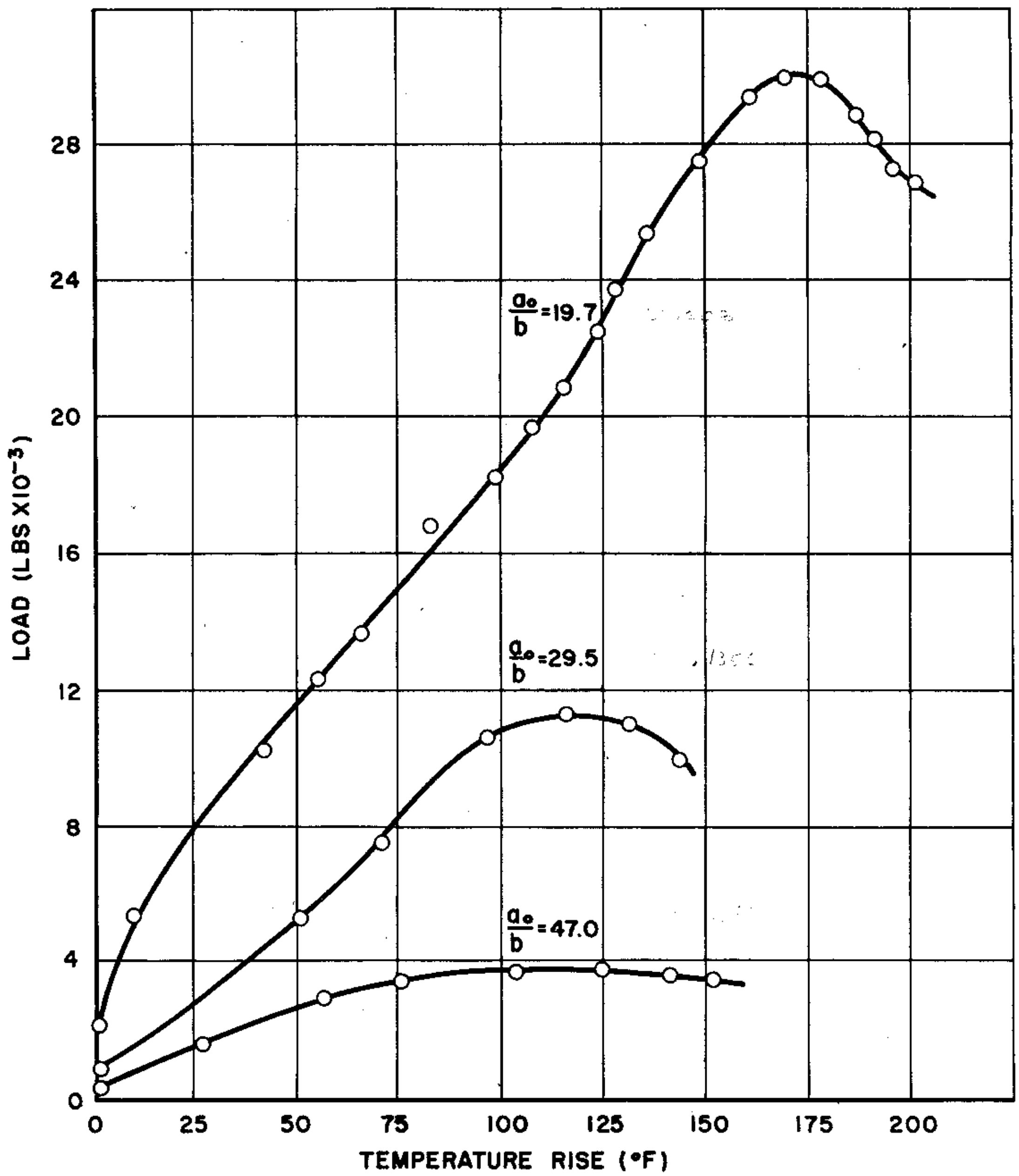

FIGURE 14 SURVEY EXPERIMENT: LOAD VS TEMPERATURE

SECTION III

EXTENSION OF ELASTIC CRITERIA TO INELASTIC BUCKLING

It has been established that the Euler buckling relation for columns is not valid for small slenderness ratios. As shown by Von Karman[11] and further by Shanley,[7] this inelastic region can be predicted for small eccentricities by use of the isothermal compressive stress-strain data. Briefly the procedure consists of:

1. Obtaining the tangent modulus as a function of the stress from these data.
2. Replacing the Young's modulus E by the tangent modulus E_t and for the average stress calculate the slenderness ratio by the Engesser relation (Ref. 7, Equation 18.2).

$$\sigma_{cr} = \frac{\pi^2 E_t}{(l/\rho)^2}$$

3. Plot the critical stress as a function of the slenderness ratio. The region of low slenderness ratios where the Engesser relation departs from the Euler relation, has been shown experimentally to be the region of inelastic behavior.

It is proposed to extend this procedure to the non-isothermal cases by using the elastic limiting load relation, equation (64), along with the long-time elevated temperature stress-strain data,[13] shown in Figure 15.* For a given temperature the average stress, tangent modulus, and secant modulus can be obtained from Figure 16. Replacing E by E_t or E_s Equation (64) can be written as

$$-\frac{N^*_{x_{cr}}}{b} = \frac{\pi^2 E_t}{12(1-\nu)^2(a_0/b)^2} = \sigma_{cr} \tag{84}$$

or

$$-\frac{N^*_{x_{cr}}}{b} = \frac{\pi^2 E_s}{12(1-\nu^2)(a_0/b)^2} = \sigma_{cr} \tag{85}$$

* The data shown is for 75S-T6 extruded aluminum alloy since, at the time of writing, data for 75S-T6 plate was not available.

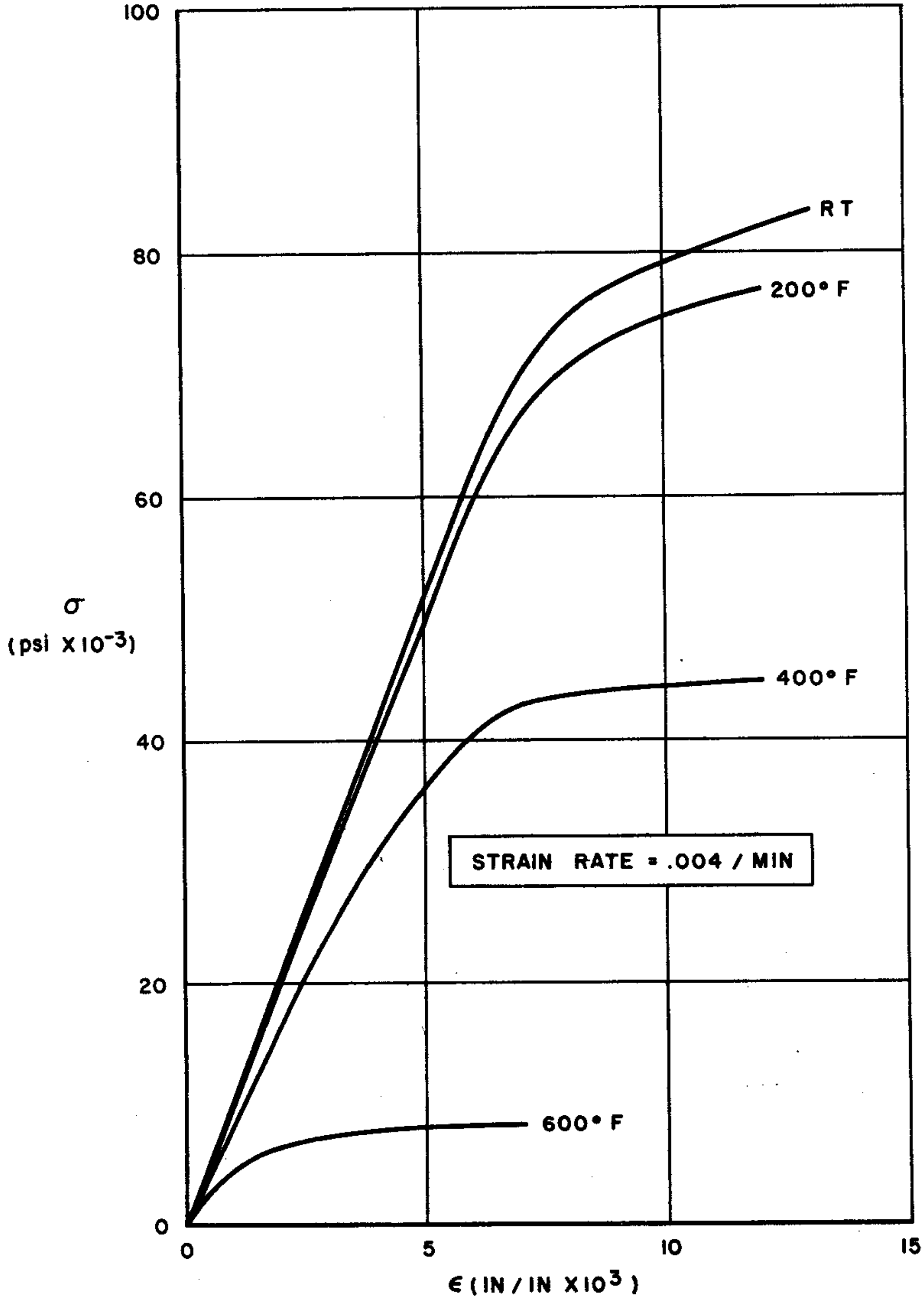

FIGURE 15 COMPRESSIVE STRESS-STRAIN DATA FOR 75S-T6 ALUMINUM ALLOY

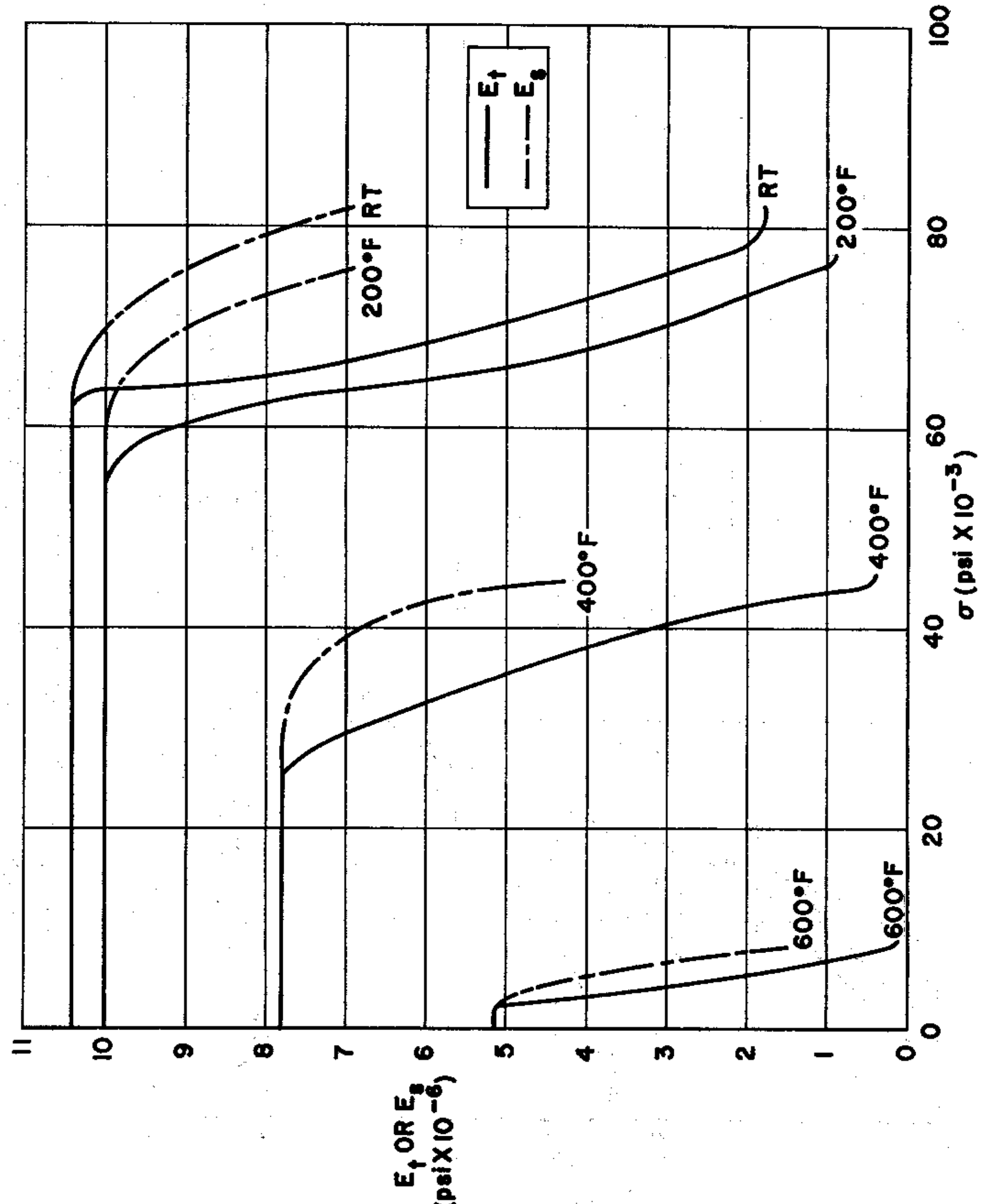

FIGURE 16 TANGENT AND SECANT MODULI VS STRESS FOR 75S-T6 ALUMINUM ALLOY

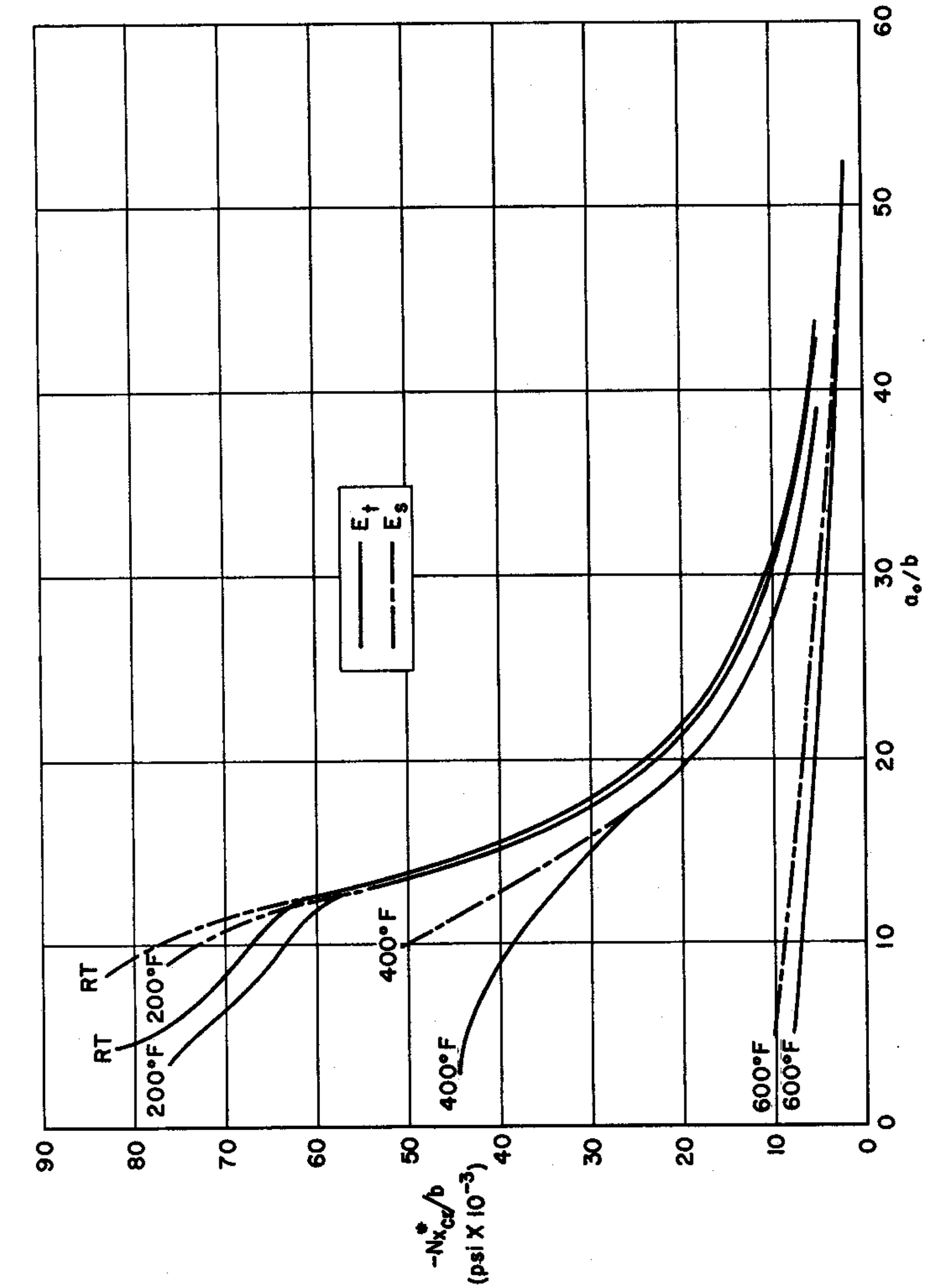

FIGURE 17 CRITICAL BUCKLING LOADS VS LENGTH TO THICKNESS RATIO FOR 75S-T6 ALUMINUM ALLOY

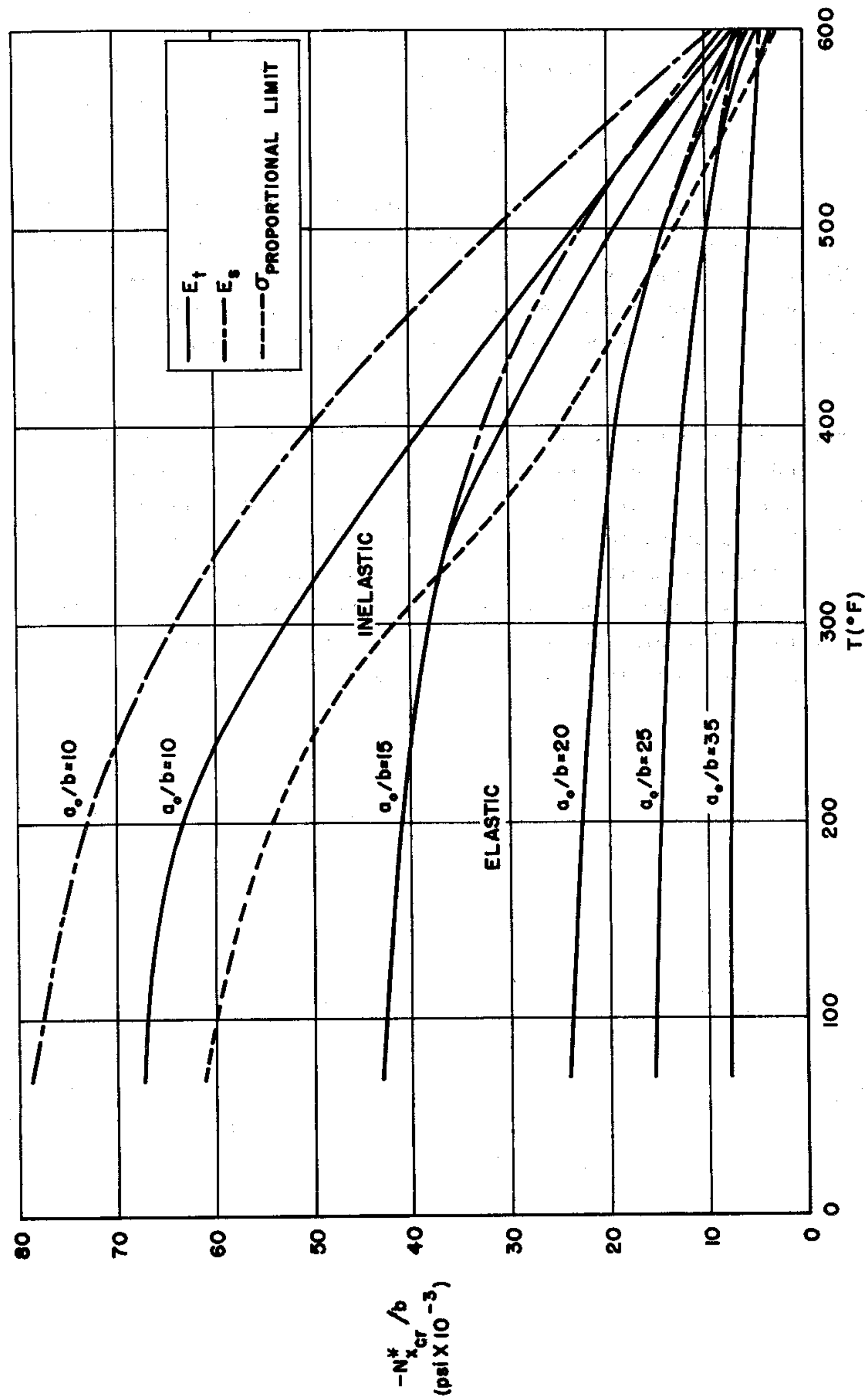

FIGURE 18 CRITICAL BUCKLING LOADS VS TEMPERATURE FOR 75S-T6 ALUMINUM ALLOY

This allows calculation of the permissible a_0/b ratio. In this manner the curves shown in Figure 17 can be constructed. Crossplotting for each a_0/b ratio allows construction of Figure 18.

For a given system, say, $a_0/b = 15$, this plot indicates the various combinations of critical stress and temperature possible for a particular material. Below approximately 310°F this plate would buckle elastically. However, when this temperature is exceeded, the buckling becomes inelastic. Curves in Figure 18 were plotted for the completely rigid constraint case ($K = \infty$).

It will be noted that both the tangent modulus and the secant modulus were used for the calculation of the critical buckling loads. This is done since it is not clear which modulus should be used. There is, in fact, considerable doubt as to the justification of the use of equations (84) and (85) for the prediction of the behavior of plates in the inelastic range. For this reason the method proposed must be restricted to (1) defining the limits of the elastic analysis and (2) determining the critical stress if this stress lies within the elastic range.

SUMMARY

A method has been presented which enables the prediction of the stresses and deflections that are the responses to a heat input in a simplified sheet-stringer panel. The heated plate equations were made tractable by the assumptions that temperature gradients exist only through the thickness of the plate and that bending occurs in only one direction. Under these simplifying assumptions relations were developed in which the stresses and transverse deflections were found in terms of the sectional forces and the thermal forces and moments. By consideration of the total expansion of the plate and the reaction of the structure external to the area of interest a relation was derived in which the thermal force can be expressed as a function of the in-plane sectional force. A semi-graphical method was devised for the calculation of stresses and transverse deflections from the surface temperatures and the thermal forces and moments. It was shown that the maximum in-plane force due to heating cannot be greater than that given by the Euler formula for flat plates in uni-axial compression.

The elastic analysis was extended to predict inelastic bending by replacing the elastic modulus by either the tangent modulus or secant modulus in the critical load equation and by introducing the elevated temperature compressive stress-strain data. A method was thereby proposed to determine the combination of average stress, dimensions, and temperatures which would produce permanent deformations.

REFERENCES

1. Ambrosio, A., Ishimoto, T., *Analytical Studies of Aircraft Structures Exposed to Transient External Heating. Volume II, Thermal Response of a Finite Plate and the "Thin" Plate Criterion.* WADC-TR 54-579, Department of Engineering, University of California at Los Angeles, November, 1954.

2. Luce, R.W., Jr., Gartland, R., Gray, E.I., *Time Dependent Thermo-Elastic Studies of Thin Skinned Construction Used in Modern Aircraft.* Allied Research Associates Document No. ARA - M- 5174, Boston, June, 1954.

3. Mahlmeister, J.E., Ishimoto, T., Ambrosio, A., *Studies on Thermal Stresses for Aircraft Structures Exposed to Transient External Heating, Vol. I, Evaluation of the Thermal Response, Force and Moment in a Plate.* Department of Engineering, University of California at Los Angeles. WADC-TR-55-192, Vol I April, 1955.

4. Nadai, A., *Elastiche Platten.* (Elastic Plates) Julius Springer, Verlag, Berlin, 1925.

5. Needham, R.A., *Permanent Buckling of Sheet Stringer Panels at Elevated Temperatures.* WADC-TR-53-209, Department of Engineering, University of California at Los Angeles, July, 1953.

6. Peery, D. J., *Aircraft Structures.* p. 369, equation 14.14, McGraw-Hill Book Co., New York, 1949.

7. Shanley, F. R., *Weight Strength Analysis of Aircraft Structures.* p. 328, McGraw-Hill Book Co., New York, 1952.

8. Timoshenko, S., *Theory of Elastic Stability.* McGraw-Hill Book Co., New York, 1936.

9. Timoshenko, S. and Goodier, J.N., *Theory of Elasticity.* Chapter XIV, p. 401, McGraw-Hill Book Co., New York, 1951.

10. Tsien, H. S., "Similarity Laws for Stressing Heated Wings." *Journal of Aero. Sci.* 20, 1-11 (1953).

11. Von Karman, T., *Investigations on Buckling Strength.* Forschungsanbeiten No. 81, Berlin, 1910.

12. Zizicas, G.A., *Transient Thermal Stresses in Thin Isotropic Elastic Plates.* Department of Engineering, University of California at Los Angeles, Report No. 52.7, April 1952.

13. Heimerl, G.J., and Roberts, W.M., *Determination of Plate Compressive Strengths at Elevated Temperatures.* NACA Report 960, Langley Aeronautical Laboratory, 1950.

DISTRIBUTION LIST

Cys	ACTIVITIES AT WPAFB
1	WCOSI-3
1	WCOSI-4
1	WCRRN
1	WCRTL
1	B. E. Gatewood Mechanics Dept., MCLI USAFIT
20	TICSC (ASTIA)
11	WCISS-1

OTHER DEPT. OF DEFENSE ACTIVITIES

Cys	
1	Chief Bureau of Aeronautics (AD-4) Department of the Navy Washington 25, D.C.
1	Director U.S. Naval Research Laboratory Attn: Mrs. Katherine Cass, Code 1501 Washington 25, D. C.
1	Chief, Bureau of Ordnance Department of the Navy Attn: Tech Library, AD-3 Washington 25, D. C.
1	Commanding Officer and Director U.S. Naval Radiological Defense Laboratory Attn: Library Branch, Code 3-222A San Francisco, California
1	Director Material Laboratory (Code 960) New York Naval Shipyard Brooklyn 1, New York
1	Commanding Officer U.S. Naval Air Development Center Attn: NADC Library Johnsville, Pa.
1	Commanding Officer U.S. Naval Air Special Weapons Facility Kirtland Air Force Base Albuquerque, New Mexico
1	Director Ballistic Research Laboratories Attn: TBL & WSL Aberdeen Proving Ground, Maryland
1	Chief of Research and Development Department of the Army Washington 25, D. C.
1	Director, Weapons Systems Evaluation Group Thru: Joint Chiefs of Staff Message Center Room 1E 884 Pentagon Washington 25, D. C.

Cys	OTHER DEPT. OF DEF. ACT. (Cont'd)
1	Director of Development Planning Headquarters, U. S. Air Force Attn: AFDAP/W Washington 25, D. C.
1 1	Classified Technical Library (For Division of Military Application) U. S. Atomic Energy Commission 1901 Constitution Avenue, N. W. Washington 25, D. C.
1	Commander in Chief Strategic Air Command Attn: Chief, Operations Analysis Offutt Air Force Base Nebraska
1	Commander Air Defense Command Attn: ADOPR-3 Ent Air Force Base Colorado Springs, Colorado
1	Hq Air Research & Development Command PO Box 1395 Attn: RDTDA Baltimore 3, Maryland
1	Director Air University Library Maxwell Air Force Base Alabama
1	DCS/Development (AFDDC-ND) Hq USAF Washington 25, D. C.
1	Commander Air Force Special Weapons Center Attn: Technical Information & Intelligence Kirtland Air Force Base, New Mexico
1	Director of Intelligence Hq. USAF Attn: AFOIN-3B Washington 25, D. C.
1	Office of Naval Research (Code 811) Navy Department Washington 25, D. C.
1	Commander Tactical Air Command Attn: Operations Analysis Directorate Langley Air Force Base, Virginia
1	Commander in Chief Strategic Air Command Attn: Chief, Operations Analysis Offutt Air Force Base Nebraska

Cys	OTHER DEPT. OF DEF. ACT. (Cont'd)
1	Commander Air Defense Command Attn: ADOPR-3 Ent Air Force Base Colorado Springs, Colorado
1	Director of Research and Development Headquarters USAF Attn: AFDRD-AN Washington 25, D. C.
1	Hq Air Research & Development Command PO Box 1395 Attn: RDTDA Baltimore, Maryland
1	Director of Development Planning Headquarters, USAF Attn: AFDAP/W Washington 25, D. C.
1	Commanding Officer Air Development Squadron FIVE NAS, Moffett Field, California
1	Chief, Armed Forces Special Weapons Project Attn: Document Library Branch Washington 25, D. C.
1	Technical Library Hq FC AFSWP Sandia Base Attn: Lt Edwin R. Turner Albuquerque, New Mexico
1	Director Office of Special Weapons Developments Continental Army Command Fort Bliss, Texas
1	Assistant for Operations Analysis Headquarters United States Air Force Washington 25, D. C.
1	Bureau of Aeronautics Gen. Rep., USN Central District Wright-Patterson AFB, Ohio
1	Commander U. S. Naval Ordnance Laboratory Attn: Library White Oak, Silver Spring, Maryland
2	Commander U. S. Air Force Academy Attn: Department of Engineering Lowry Air Force Base, Colorado

Cys	OTHER U.S. GOVERNMENT AGENCIES
1	Los Alamos Scientific Laboratory Attn: Dr. Harold Agnew PO Box 1663 Los Alamos, New Mexico
1	National Advisory Comm. for Aeronautics Attn: Eugene B. Jackson Chief, Div. of Research Information 1512 H. Street, N. W. Washington 25, D. C.
1	National Advisory Comm. for Aeronautics Langley Aeronautical Laboratory Attn: Mr. P. Donely and Dr. John Duberg Langley Air Force Base, Virginia

Cys	NON-GOVERNMENT INDIVIDUALS AND ORGANIZATIONS
50	Prof. W. C. Hurty University of California Department of Engineering PO Box 24063 Los Angeles 24, California
1	Massachusetts Institute of Technology Department of Aeronautical Engineering Attn: Dr. Emmett A. Witmer, Rm 41-219 Cambridge 39, Massachusetts
1	Allied Research Associates, Inc. Attn: Mr. Lawrence Levy, President 43 Leon Street Boston 15, Massachusetts
1	The RAND Corporation Attn: Dr..E. H. Plesset 1700 Main Street Santa Monica, California
1	Vitro Laboratories (Div. of the Vitro Corporation of America) Attn: Library 200 Pleasant Valley Way West Orange, New Jersey
1	Bell Aircraft Corporation Attn: Mrs. Jasmine H. Mulcahey PO Box 1 Buffalo 5, New York
1	Boeing Airplane Company Seattle Division Attn: George C. Martin Chief Engineer Seattle 14, Washington
1	Chance Vought Aircraft, Inc. Attn: Mr. P. C. Moran, Supervisor Engineering Office PO Box 5907 Dallas, Texas
1	CONVAIR A division of General Dynamics Corp. Attn: Dora B. Burke, Engineering Librarian San Diego, California
1	R. H. Widmer Assistant Chief Engineer Douglas Aircraft Company, Inc. 2000 No. Memorial Boulevard Tulsa, Oklahoma
1	Douglas Aircraft Company, Inc. Long Beach Division Attn: C. C. Wood, Chief Engineer 3955 Lakewood Blvd Long Beach, California
1	Grumman Aircraft Engineering Corp. Attn: Mrs. A. M. Gray Bethpage, Long Island, New York
1	Lockheed Aircraft Corp. Factory "A", Plant A-1 Attn: J. F. McBrearty - 63/3 2555 No. Hollywood Way Burbank, California

Cys	NON-GOVERNMENT INDIVIDUALS AND ORGANIZATIONS (Cont'd)
1	The Glenn L. Martin Company Attn: Mrs. Mary R. Ezzo Engineering Librarian Baltimore 3, Maryland
1	McDonnell Aircraft Corp. Attn: Engineering Library - Dept 204 PO Box 516 St. Louis, Missouri
1	North American Aviation, Inc., Los Angeles International Airport Attn: D. H. Mason Engineering Technical File Los Angeles 45, California
1	Northrop Aircraft, Inc. Northrop Field Attn: R. P. Jackson Hawthorne, California
1	Mrs. Helen Stieglitz, Librarian Engineering Department Republic Aviation Corp. Farmingdale, New York
1	Cook Research Laboratories Division 8100 No. Monticello Ave. Attn: Mr. R. C. Edwards, Business Mgr. Skokie, Illinois
1	Operations Research Office The Johns Hopkins University Attn: Library 7100 Connecticut Ave. Chevy Chase, Maryland
1	Division of Research University of Dayton Attn: E. A. Janning, Administrator 300 College Park Avenue Dayton 9, Ohio
1	The Applied Physics Laboratory Johns Hopkins University Attn: Technical Reports Office 8621 Georgia Avenue Silver Spring, Maryland
1	Beverly W. Hodges Chief of Structural Staff Boeing Amrplane Company Wichita Division Wichita, Kansas
1	Dr. E. E. Sechler California Institute of Technology Pasadena, California
1	Professor Bruno A. Boley Dept. of Civil Engrg. & Engrg. Mechanics Columbia University New York 27, New York
1	New York University College of Engineering Attn: Prof. Fred Landis, Dept. of Mechanical Engrg. New York 53, New York
1	Aerophysics Development Corporation Attn: Mr. A. T. Zahorski 924 Anacapa St. Santa Barbara, California